Direction of Arrival Estimation via Joint Sparse Bayesian Learning for Bi-Static Passive Radar

XINYU ZHANG, **KAI HUO**, **YONGXIANG LIU**, **AND XIANG LI**
College of Electronic Science and Engineering, National University of Defense Technology, Changsha 410073, China
Corresponding author: Kai Huo (huokai2001@163.com)

ABSTRACT Direction-of-arrival (DOA) estimation using sparsity-inducing techniques has attracted much interest recently. In this paper, the DOA estimation for the bi-static passive radar is investigated. Under the framework of sparse Bayesian learning (SBL), a joint sparse Bayesian model is established to combine the measurements from both stations and yield improved targets DOA estimation. First, the maximum *a posteriori* (MAP) estimation of the DOA using the joint data set is derived. With the utilization of more measurements, the joint reconstruction process can produce far more precise estimates. To reduce the computational expense, a fast SBL method based on evidence maximization is also proposed. Using the fix-point method, the fast SBL method tends to converge faster than the MAP estimator. Theoretical results focusing on local convergence property of the fast SBL method are provided. The simulation results show that the proposed methods outperform the conventional SBL methods, especially in harsh scenarios with a limited number of snapshots and low signal-to-noise ratio (SNR).

INDEX TERMS Direction-of-arrival estimation, sparse Bayesian learning, bi-static passive radar.

I. INTRODUCTION

Direction of arrival estimation has been a hot topic in signal processing for several decades [1]–[4]. It is an essential problem in Radar, Sonar and seismic sensing etc.. Sub-space based methods [5]–[8], such as Multiple Signal Classification (MUSIC) [5], were proposed based on the premise that the targets signals only span a low dimensional subspace. These methods were able to achieve super-resolution within a Rayleigh cell, but usually require moderate SNR, non-coherent sources assumption and sufficient number of snapshots, which confines their application in practice. Besides the sub-space methods, a family of parametric methods based on the maximum likelihood (ML) paradigm [9] enjoy excellent statistical properties. However, the heavy computational burden has prohibited such methods from practical application.

Recently, Sparsity-inducing techniques have been introduced into DOA estimation and achieve great success in improving robustness of estimation against noise, limited number of snapshots, and correlation of signals. The topic

has attracted much interest in the last few decades and continues drawing attention. In its most basic form, the sparsity-inducing models introduce an over-complete dictionary for signal representation which makes the corresponding weight vector sparse, i.e. the non-zero rows are much less than the zero ones. Because of the over-complete dictionary, this problem is ill-posed unless further constraints are established. One class of the methods solve the problem by inducing l_p-norm penalty into the minimizing objective function [10]–[13]. However, imposing l_p-norm penalty with $p < 1$ for sparsity usually causes a combinatorial increase in local optima [14]. Finding such local optima may be too computationally expensive to afford for some practical systems. Later the sparsity-inducing model was expanded to utilize multiple measurement vectors (MMV) for DOA estimation. In the new model, it is reasonably assumed that all vectors sampled from different time share a common sparsity profile. The row-wise l_2-norm can be utilized to combine multiple snapshots and form a single sparse vector [15]–[17]. Then the algorithms developed for single measurement vector, such as the Least Absolute Shrinkage and Selection Operator (LASSO) [18], can be extended to fit the new model. Other variants included using row-wise l_1-norm [19] or row-wise l_∞-norm [20] for

signal sparsity constraints. Such convex relaxing techniques made the DOA estimation accessible by the established convex-programming but scarified the recovery performance, i.e. the results may not be sufficiently sparse.

Another class of the sparsity constrained methods called sparse Bayesian learning approach the problem from the Bayesian perspective. There are two types of estimation in this category. Type-I estimation is equivalent to MAP estimation using a sparsity-inducing prior distribution. Type-II estimation operates in latent variable space leveraging a variational representation of the latent variable distribution which leads to sparse estimators reflecting posterior information beyond the mode [21]. Recently, a bunch of algorithms based on this method have been proposed for different scenarios [22]–[25]. Theoretical results show that Type-II estimator could hold several desirable advantages over all possible Type-I estimators with most,and in certain quantifiable conditions all, local optima smoothed away [21].

In this paper, we investigate how to jointly use measurements from bi-static passive radar for DOA estimation. Investigation of techniques used in passive radar [26]–[28] has been extensively conducted for decades due to its several advantages over active radar. In the last few years, the interest in target detection and tracking based on bi-static or multi-static radar has significantly grown up [29]–[32]. In [33], a SBL based method with grid refining strategy was proposed to obtain joint direction of departure and direction of arrival estimation for bi-static multiple-input multiple-output (MIMO) radar. In the method, atoms of the dictionary matrix were formed by the Kronecker product of the steering vector of transmitting array and the steering vector of receiving array. However, such method did not take full advantage of the geometry relations of the bi-static system, e.g. the range estimates of targets. In [34], the ML solution of target localization was derived for multi-static passive arrays under various assumptions on relative source spectral information. To the authors best knowledge, using SBL to jointly estimate the targets' DOA for bi-static passive radar, has rarely been studied in the open literatures, yet it is quite useful in practice. Bi-static passive radar is consisted of two stations that only receive data from source emitters. Here the joint estimation means combining measurements from the two receiving arrays to yield improved estimates. The angles of arrival for these two arrays are closely linked to each other by a one-to-one mapping determined by the bi-static geometry. It is this link that the proposed method uses to jointly learn the DOA of targets under the SBL framework. If we directly average the estimated angles from each station, the result would be less precise than the best estimate of those two. However, by using SBL, we can achieve improved estimation. The target localization using bi-static or multi-static passive radar can find many applications in practice [36], [37]. For example, the WiFi-based antenna arrays, such as indoor routers, can be employed to form a bi-static or multi-static radar for detecting and tracking people moving inside a building, for tracking vehicles moving in a parking area or for the
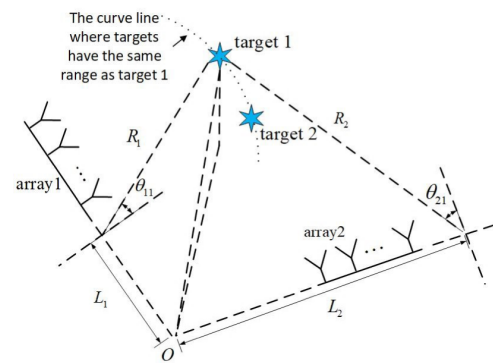

FIGURE 1. Geometry of the bi-static system.

surveillance of sensible areas within railway station, airport terminals and private commercial premises [38], [39].

The main contribution of this paper can be divided into three aspects. Firstly, a joint sparse Bayesian model is established to combine the measurements from both stations and the MAP estimator of targets DOA was derived with expectation maximization (EM) technique [40]. It was found that using the data from bi-static system could help enhance the uniqueness condition for reconstruction process. However, it was found that although the MAP estimator based on EM could achieve optimal performance in Bayesian perspective, the computational expense would be unbearable in some practical situations. Therefore, based on the fix-point method and appropriate approximation, we then developed a fast optimization algorithm that maximize a Type-II Gaussian likelihood function. In addition, the local convergence property of this algorithm was given and proved theoretically. In our experiments, we show that in the case of low SNR and limited number of snapshots, the proposed SBL algorithms could achieve lower Root-Mean-Squared-Error (RMSE) than the conventional methods that only used data from either station.

The rest of this paper is organized as follows. In Section II, we give a description of the signal model. For the joint DOA estimation, the bi-static geometry is utilized. We show that under the Bayesian framework, the measurements from two radar stations can be combined to obtain the DOA estimation. Then in Section III, we derive an iterative algorithm using EM technique for the DOA estimation model. We then develop a fast algorithm in Section IV by maximizing a Type-II evidence function. In Section V, we present the simulation results of the proposed method and comparison with the conventional methods. Finally, Section VI concludes the paper.

II. SIGNAL MODEL
A. SYSTEM MODEL
Consider a bi-static passive radar that consists of two linear phased arrays located at separate places. Here we assume the two arrays are placed in the same plane. The geometry of the bi-static system is depicted by Fig 1. Denote the cross point of lines along the arrays as O. The distance between station 1 and the cross point is L_1 and the distance between station 2 and the cross point is L_2. Assume that the first array consists

of M_1 sensors separated by d_1 and the second array consists of M_2 sensors separated by d_2. K far-field independent sources are incident on the radar. Here we assume they are located within the same range bin of radar, because it is usually required for DOA estimation that the utilized measurements contain all the target signals but samples from different range bins may not meet such requirement. Denote the range of targets perceived by station 1 as R_1 and the range with respect to station 2 is R_2. The incident angles with respect to the boresight of station 1 are denoted as $\theta_1 = [\theta_{11}\ \theta_{12}\ \cdots\ \theta_{1K}]^T$ and the incident angles are $\theta_2 = [\theta_{21}\ \theta_{22}\ \cdots\ \theta_{2K}]^T$ with respect to the boresight of station 2 where $(\cdot)^T$ represents the matrix transpose. It can be easily found through simple analysis of the geometry that θ_{1i} and θ_{2i} for $i = 1, 2, \cdots, K$ are linked by

$$L_2^2 + R_2^2 - 2\cos(\theta_{2i} + \frac{\pi}{2}) = R_1^2 + L_1^2 - 2\cos(\frac{\pi}{2} - \theta_{1i}) \quad (1)$$

where the angles of arrival are in the range $[-\frac{\pi}{2}, \frac{\pi}{2}]$. Further simplification of (1) gives

$$\theta_{2i} = -\arcsin(\frac{L_2^2 + R_2^2 + 2R_1L_1\sin\theta_{1i} - R_1^2 - L_1^2}{2R_2L_2}) \quad (2)$$

From (2), we can see that such link is dependent on R_1 and R_2 which are usually measured in the stage of detection. In many practical applications, e.g. wide-band radar, the precision of range measurement is higher than the angle estimation. The received signals at station 1 and station 2 can be written as

$$\mathbf{Y}_1 = \mathbf{A}_1\mathbf{S}_1 + \mathbf{N}_1$$
$$\mathbf{Y}_2 = \mathbf{A}_2\mathbf{S}_2 + \mathbf{N}_2 \quad (3)$$

where $\mathbf{Y}_1 = [\mathbf{y}_1(1)\ \mathbf{y}_1(2)\ \cdots\ \mathbf{y}_1(L)]$ is a $M_1 \times L$ matrix of the received data at station 1 collected from L samples, $\mathbf{Y}_2 = [\mathbf{y}_2(1)\ \mathbf{y}_2(2)\ \cdots\ \mathbf{y}_2(L)]$ is a $M_2 \times L$ matrix of the received data at station 2 and

$$\mathbf{A}_1 = [\mathbf{a}(\theta_{11})\ \mathbf{a}(\theta_{12})\ \cdots\ \mathbf{a}(\theta_{1K})]$$
$$\mathbf{A}_2 = [\mathbf{a}(\theta_{21})\ \mathbf{a}(\theta_{22})\ \cdots\ \mathbf{a}(\theta_{2K})] \quad (4)$$

where $\mathbf{a}(\theta) = [1\ e^{j2\pi\frac{d}{\lambda}\sin(\theta)}\ \dots\ e^{j2\pi(M-1)\frac{d}{\lambda}\sin(\theta)}]^T$ is the array manifold and λ is the wavelength of the sources, M is the number of array elements. $\mathbf{S}_1$ and $\mathbf{S}_2$ are the complex amplitudes of the targets sampled at L different time. $\mathbf{N}_1$ and $\mathbf{N}_2$ are the white Gaussian noise from the first array and the second array respectively. Conventional DOA estimation methods based on sub-space decomposition usually requires estimation of the covariance matrix:

$$\mathbf{R}_1 = \frac{1}{L}\mathbf{Y}_1\mathbf{Y}_1^H, \mathbf{R}_2 = \frac{1}{L}\mathbf{Y}_2\mathbf{Y}_2^H \quad (5)$$

where $(\cdot)^H$ represents the conjugate transpose, and sub-space decomposition by eigenvalue decomposition [41]:

$$\mathbf{R}_1 = \mathbf{U}_{s1}\Lambda_{\mathbf{s}1}\mathbf{U}_{s1}^H + \frac{1}{\sigma_1^2}\mathbf{U}_{n1}\mathbf{U}_{n1}^H$$
$$\mathbf{R}_2 = \mathbf{U}_{s2}\Lambda_{\mathbf{s}2}\mathbf{U}_{s2}^H + \frac{1}{\sigma_2^2}\mathbf{U}_{n2}\mathbf{U}_{n2}^H \quad (6)$$

where $\mathbf{U}_{si}, i = 1, 2$ consist of eigenvectors of signal sub-space and $\mathbf{U}_{ni}, i = 1, 2$ consist of eigenvectors of noise sub-space, σ_1^2 and σ_2^2 are noise power of the arrays. Therefore, from (5) and (6), we can see that the performance of such methods are sensitive to limited number of samples and SNR.

B. SPARSE SIGNAL MODEL

The sparse signal model introduces an over-complete dictionary matrix $\Phi = [\mathbf{a}(\bar{\theta}_1)\ \mathbf{a}(\bar{\theta}_2)\ \cdots\ \mathbf{a}(\bar{\theta}_N)]$ into the expression of received data. Here $\bar{\theta}_i, i = 1, \cdots, N$ is a discrete sampling of spatial angle space. Then the received data can be rewritten as

$$\mathbf{Y}_1 = \Phi_1\bar{\mathbf{S}}_1 + \mathbf{N}_1$$
$$\mathbf{Y}_2 = \Phi_2\bar{\mathbf{S}}_2 + \mathbf{N}_2 \quad (7)$$

where Φ_1 and Φ_2 are the dictionary matrices for station 1 and station 2 respectively. Since we have $N \gg \max(M_1, M_2)$, the problem we face is ill-posed unless the weight matrices $\bar{\mathbf{S}}_1$ and $\bar{\mathbf{S}}_2$ are K-sparse for each column meaning only K elements corresponding to the targets directions potentially have non-zero values and every column share the same sparsity profile. To jointly exploit the received data from both stations, we relate the sampling grids $\{\bar{\theta}_{1i}\}_{i=1}^N$ of Φ_1 to the sampling grids $\{\bar{\theta}_{2i}\}_{i=1}^N$ of Φ_2 using (2). Note that the sampling grids can not be too dense, otherwise the computation expense would be unaffordable. The optimal design of joint grid maps is a interesting topic for the future research and currently out of the scope of this paper. But generally we could let either $\{\bar{\theta}_{1i}\}_{i=1}^N$ or $\{\bar{\theta}_{2i}\}_{i=1}^N$ uniformly spans the range $[-\frac{\pi}{2}, \frac{\pi}{2}]$ and the other is calculated by (2).

The probabilistic distribution of data given the weight matrix is complex Gaussian as

$$p(\mathbf{Y}_1\,|\,\bar{\mathbf{S}}_1, \sigma_1^2) = \frac{\exp\left(-\frac{1}{\sigma_1^2}\left\|\mathbf{Y}_1 - \Phi_1\bar{\mathbf{S}}_1\right\|_{\mathcal{F}}^2\right)}{(\pi\sigma_1^2)^{M_1L}}$$

$$p(\mathbf{Y}_2\,|\,\bar{\mathbf{S}}_2, \sigma_2^2) = \frac{\exp\left(-\frac{1}{\sigma_2^2}\left\|\mathbf{Y}_2 - \Phi_2\bar{\mathbf{S}}_2\right\|_{\mathcal{F}}^2\right)}{(\pi\sigma_2^2)^{M_2L}} \quad (8)$$

where $\|\cdot\|_{\mathcal{F}}$ stands for the Frobenius norm of matrix. For the prior, note that we have made connection between Φ_1 and Φ_2, therefore, it is reasonable to assume that the elements along each row of $\bar{\mathbf{S}}_1$ and $\bar{\mathbf{S}}_2$ are independent identically distributed (iid) and subject to a zero-mean complex Gaussian distribution with variance $\gamma_i \geq 0, i = 1, \cdots, N$. The elements of each column are assumed to be independent from each other. Then we can put the prior distribution of weight matrices as

$$p(\bar{\mathbf{S}}_1\,|\,\gamma) = \prod_{i=1}^L \mathcal{CN}(\mathbf{0}, \Gamma)$$

$$p(\bar{\mathbf{S}}_2\,|\,\gamma) = \prod_{i=1}^L \mathcal{CN}(\mathbf{0}, \Gamma) \quad (9)$$

where $\gamma = [\gamma_1 \ \gamma_2 \cdots \gamma_N]$ and $\Gamma = \text{diag}(\gamma)$. The variances γ are called hyper-parameters that control the sparsity of the model. In this paper, it is assumed that the variances of the target signal received by the two stations are the same. In practice, the signal variance corresponds to the signal power. The ratio of the signal power in the two stations can be estimated by the radar function. Then the received data can be compensated to make the variance of the target signal at both stations equal. When $\gamma_i = 0$, the corresponding complex amplitudes equal zero with probability 1. Thus the estimation of targets direction depends on the estimation of γ instead of the weight matrices which amounts to significantly reduction of parameters needed to be estimated.

The prior of the hyper-parameters is usually assumed to be non-informative or uniform. Using such broad prior over the hyper-parameters allows the posterior probability mass to concentrate at very small values of some of these γ variables, with the consequence that the posterior probability of the associated weights will be concentrated at zero, thus effectively 'switching off' the corresponding inputs [42]. Here we assume that the hyper-parameters are subject to Gamma distribution:

$$p(\gamma) = \prod_{i=1}^{N} \text{Gamma}(\gamma_i \mid 1, a)$$
$$p(\beta_1) = \text{Gamma}(\beta_1 \mid 1, b)$$
$$p(\beta_2) = \text{Gamma}(\beta_2 \mid 1, c) \tag{10}$$

where $\beta_1 = \sigma_1^{-2}$, $\beta_2 = \sigma_2^{-2}$ and $\text{Gamma}(x \mid \bar{a}, \bar{b}) = \Gamma(\bar{a})^{-1}\bar{b}^{\bar{a}}x^{\bar{a}-1}e^{-\bar{b}x}$ with $\Gamma(\bar{a})$ being the gamma function. In order to make the prior non-informative, we set $a \to 0$, $b \to 0$ and $c \to 0$. Empirical evidences have shown that the SBL method is robust to the choice of a, b, c, as long as their values are sufficiently small [25].

One way to obtain estimation of the hyper-parameters is by MAP estimation. On the other hand, from Bayes' theorem, the posterior distribution for γ and β_1, β_2 is given by

$$p(\gamma, \beta_1, \beta_2 \mid \mathbf{Y}_1, \mathbf{Y}_2) \propto p(\mathbf{Y}_1, \mathbf{Y}_2 \mid \gamma, \beta_1, \beta_2)p(\gamma, \beta_1, \beta_2) \tag{11}$$

Therefore, if the prior is relatively flat, in the evidence framework, the values of γ, β_1, β_2 can be obtained by maximizing the marginal likelihood function $p(\mathbf{Y}_1, \mathbf{Y}_2 \mid \gamma, \beta_1, \beta_2)$ which will be explored in Section IV.

The algorithms we proposed in this paper can still work even if the targets are off the grid, but the performance will deteriorate. However, a simple grid refinement strategy [15] can be employed to alleviate such effect. Therefore, in the derivation of our algorithms, we will omit the discussion of handling the off-grid gap.

C. UNIQUENESS OF SOLUTION IN NOISELESS CASE
Denote spark($\cdot$) as the minimal number of coherent columns of a matrix and the term diversity represents the number of elements or rows of a matrix that are not equal to zero, then the following theorem holds:

Theorem 1: Assume that spark(Φ_1) $= m_1$, spark(Φ_2) $= m_2$ and there exists a solution of $\bar{\mathbf{S}}_1$ and $\bar{\mathbf{S}}_2$ that satisfies (7) with diversity being $p < \max(m_1, m_2)/2$, then there can be no other solutions with diversity $r < \max(m_1, m_2) - p + 1$.

The proof of the theorem is provided in Appendix A. Readers can find more discussion of the uniqueness of sparse recovery solution in [17], [35]. The spark($\cdot$) corresponds to the Unique Representation Property (URP) in single-task compressive sensing problems. The theorem tells that if a solution with diversity less than $\max(m_1, m_2)/2$, is found, this solution is unique. In addition, the theorem also gives the maximum number of targets that can be uniquely estimated. It can be found that compared with the DOA estimation using data from only one station, the model diversity constraint is more relaxed in our case. Therefore, the joint reconstruction process using data from both stations helps enhance the uniqueness of the solution.

III. MAP ESTIMATION OF TARGETS DOA
In this section, we derive an iterative algorithm for DOA estimation based on standard EM technique. The algorithm proposed exploit the data from both stations instead of either one of them as in the original EM algorithms. Therefore, we denote this proposed algorithm as Bi-static Multi-snapshot Expectation Maximization (BM-EM). Following the standard SBL procedure, we will derive the estimator for hyper-parameters γ, β_1, β_2. Although the DOA estimation is only related to γ, the estimation of other hyper-parameters do affect the performance of DOA estimation. The estimation of hyper-parameters is obtained through MAP estimation:

$$(\gamma^\star, \beta_1^\star, \beta_2^\star) = \underset{\gamma, \beta_1, \beta_2}{\arg\max} \, p(\gamma, \beta_1, \beta_2 \mid \mathbf{Y}_1, \mathbf{Y}_2) \tag{12}$$

Then with the optimal hyperparameters, the MAP estimate of $\bar{\mathbf{S}}_1$ and $\bar{\mathbf{S}}_2$ can be obtained by

$$(\bar{\mathbf{S}}_1^\star) = \underset{\bar{\mathbf{S}}_1}{\arg\max} \, p(\bar{\mathbf{S}}_1 \mid \mathbf{Y}_1; \gamma^\star, \beta_1^\star)$$
$$(\bar{\mathbf{S}}_2^\star) = \underset{\bar{\mathbf{S}}_2}{\arg\max} \, p(\bar{\mathbf{S}}_2 \mid \mathbf{Y}_2; \gamma^\star, \beta_2^\star) \tag{13}$$

According to Bayes' theorem, we have

$$p(\gamma, \beta_1, \beta_2, \mathbf{Y}_1, \mathbf{Y}_2) = p(\gamma, \beta_1, \beta_2 \mid \mathbf{Y}_1, \mathbf{Y}_2)p(\mathbf{Y}_1\mathbf{Y}_2) \tag{14}$$

Ignoring irrelevant terms, (12) is equivalent to

$$(\gamma^\star, \beta_1^\star, \beta_2^\star) = \underset{\gamma, \beta_1, \beta_2}{\arg\max} \, (\ln p(\gamma, \beta_1, \beta_2, \mathbf{Y}_1, \mathbf{Y}_2)) \tag{15}$$

A. E-STEP
To obtain the objective function in (15), we need to compute the following integral:

$$\ln p(\gamma, \beta_1, \beta_2, \mathbf{Y}_1, \mathbf{Y}_2)$$
$$= \ln \iint p(\gamma, \beta_1, \beta_2, \bar{\mathbf{S}}_1, \bar{\mathbf{S}}_2, \mathbf{Y}_1, \mathbf{Y}_2) \, d\bar{\mathbf{S}}_1 \, d\bar{\mathbf{S}}_2 \tag{16}$$

However, optimizing the right side of (16) usually leads to a problem that is analytically intractable. Therefore, we need to

build a tight lower bound of $\ln p(\gamma, \beta_1, \beta_2, \mathbf{Y}_1, \mathbf{Y}_2)$. With the Jensen's inequality, a tight lower bound can be given as [25]

$$
\begin{aligned}
&\mathcal{L}(\gamma, \beta_1, \beta_2)\\
&\triangleq \langle \ln p(\gamma, \beta_1, \beta_2, \overline{\mathbf{S}}_1, \overline{\mathbf{S}}_2, \mathbf{Y}_1, \mathbf{Y}_2) \rangle_{p(\overline{\mathbf{S}}_1, \overline{\mathbf{S}}_2 \mid \gamma, \beta_1, \beta_2, \mathbf{Y}_1, \mathbf{Y}_2)}
\end{aligned}
\tag{17}
$$

where $\langle \cdot \rangle_{p(x)}$ is the expectation operator with respect to the distribution $p(x)$. For further derivation, we need to evaluate the posterior distribution of $\overline{\mathbf{S}}_1, \overline{\mathbf{S}}_2$. According to Bayes' theorem, we have

$$
\begin{aligned}
&p(\overline{\mathbf{S}}_1, \overline{\mathbf{S}}_2 \mid \gamma, \beta_1, \beta_2, \mathbf{Y}_1, \mathbf{Y}_2)\\
&\quad \propto p(\mathbf{Y}_1, \mathbf{Y}_2 \mid \gamma, \beta_1, \beta_2, \overline{\mathbf{S}}_1, \overline{\mathbf{S}}_2) p(\overline{\mathbf{S}}_1, \overline{\mathbf{S}}_2 \mid \gamma, \beta_1, \beta_2)
\end{aligned}
\tag{18}
$$

Here we assume that $\overline{\mathbf{S}}_1$ and $\overline{\mathbf{S}}_2$ are independent from each other. In practice, there could be many factors that contribute to this assumption [34]. Although the signals share the same sources, they are attenuated and also modulated during transmission. Turbulence of the transmission channel is one of the factors that make them incoherent. Furthermore, the signals for DOA estimation are already down-converted to the base band. Therefore, the turbulence in the radar system could also contribute to the assumption. With this assumption and that the noise in the two stations are independent, we have $\mathbf{Y}_1$ and $\mathbf{Y}_2$ are also independent from each other. Therefore, we have

$$
\begin{aligned}
&p(\overline{\mathbf{S}}_1, \overline{\mathbf{S}}_2 \mid \gamma, \beta_1, \beta_2, \mathbf{Y}_1, \mathbf{Y}_2)\\
&\quad = p(\overline{\mathbf{S}}_1 \mid \gamma, \beta_1, \mathbf{Y}_1) p(\overline{\mathbf{S}}_2 \mid \gamma, \beta_2, \mathbf{Y}_2)
\end{aligned}
\tag{19}
$$

Since Gaussian distribution is self-conjugate, the posterior distribution of $\overline{\mathbf{S}}_i, i = 1, 2$ is also Gaussian. Combining (8) and (9) gives

$$
\begin{aligned}
&p(\overline{\mathbf{S}}_1 \mid \gamma, \beta_1, \mathbf{Y}_1)\\
&= \frac{\exp\left(-\operatorname{tr}\left((\overline{\mathbf{S}}_1 - \mu_{\overline{\mathbf{S}}_1})^H \Sigma_{\overline{\mathbf{S}}_1}^{-1}(\overline{\mathbf{S}}_1 - \mu_{\overline{\mathbf{S}}_1})\right)\right)}{(\pi^N \det(\Sigma_{\overline{\mathbf{S}}_1}))^L}
\end{aligned}
\tag{20}
$$

where $\operatorname{tr}(\cdot)$ represents the trace of a matrix, $(\cdot)^{-1}$ is matrix inversion, $\det(\cdot)$ is the determinant of matrix and

$$
\begin{aligned}
&p(\overline{\mathbf{S}}_2 \mid \gamma, \beta_2, \mathbf{Y}_2)\\
&= \frac{\exp\left(-\operatorname{tr}\left((\overline{\mathbf{S}}_2 - \mu_{\overline{\mathbf{S}}_2})^H \Sigma_{\overline{\mathbf{S}}_2}^{-1}(\overline{\mathbf{S}}_2 - \mu_{\overline{\mathbf{S}}_2})\right)\right)}{(\pi^N \det(\Sigma_{\overline{\mathbf{S}}_2}))^L}
\end{aligned}
\tag{21}
$$

where posterior mean $\mu_{\overline{\mathbf{S}}_1}, \mu_{\overline{\mathbf{S}}_2}$ and covariance $\Sigma_{\overline{\mathbf{S}}_1}, \Sigma_{\overline{\mathbf{S}}_2}$ can be written as

$$
\begin{aligned}
\mu_{\overline{\mathbf{S}}_1} &= \beta_1 \Sigma_{\overline{\mathbf{S}}_1} \Phi_1^H \mathbf{Y}_1 \quad \mu_{\overline{\mathbf{S}}_2} = \beta_2 \Sigma_{\overline{\mathbf{S}}_2} \Phi_2^H \mathbf{Y}_2\\
\Sigma_{\overline{\mathbf{S}}_1}^{-1} &= \beta_1 \Phi_1^H \Phi_1 + \gamma^{-1} \quad \Sigma_{\overline{\mathbf{S}}_2}^{-1} = \beta_2 \Phi_2^H \Phi_2 + \gamma^{-1}
\end{aligned}
\tag{22}
$$

Now we have all the ingredients for the optimization problem in (15). In the next subsection, we will continue derivation for the update of hyperparameters.

B. M-STEP

In this subsection, we address the estimation of hyperparameters γ, β_1, β_2. The estimation is done by maximizing the objective function in (17), following a similar procedure in [25]. However, because in our algorithm, the data from two stations are jointly utilized, the update for γ is different.

The estimation of β_1 and β_2 is only dependent on data from either station 1 or station 2. Thus, their estimation is the same as in [25] and we give the update of β_1 and β_2 directly as follows

$$
\beta_1 = \frac{M_1 L}{\left\|\mathbf{Y}_1 - \Phi_1 \mu_{\overline{\mathbf{S}}_1}\right\|_{\mathcal{F}}^2 + L \operatorname{tr}(\Phi_1 \Sigma_{\overline{\mathbf{S}}_1} \Phi_1^H)}
\tag{23}
$$

and

$$
\beta_2 = \frac{M_2 L}{\left\|\mathbf{Y}_2 - \Phi_2 \mu_{\overline{\mathbf{S}}_2}\right\|_{\mathcal{F}}^2 + L \operatorname{tr}(\Phi_2 \Sigma_{\overline{\mathbf{S}}_2} \Phi_2^H)}
\tag{24}
$$

where we have omitted the prior distribution of β_1 and β_2, as the prior distribution is non-informative when $b \to 0$ and $c \to 0$. The above equation is obtained by directly taking differentiation of (17) over β_1 and β_2 and setting them to zero. In other literatures, the following update rule for noise variance was also used [42], [43]:

$$
\begin{aligned}
\beta_1 &= \frac{M_1 - N + \sum_{i=1}^{N} \frac{(\Sigma_{\overline{\mathbf{S}}_1})_{i,i}}{\gamma_i}}{\left\|\mathbf{Y}_1 - \Phi_1 \mu_{\overline{\mathbf{S}}_1}\right\|_{\mathcal{F}}^2}\\
\beta_2 &= \frac{M_2 - N + \sum_{i=1}^{N} \frac{(\Sigma_{\overline{\mathbf{S}}_2})_{i,i}}{\gamma_i}}{\left\|\mathbf{Y}_2 - \Phi_2 \mu_{\overline{\mathbf{S}}_2}\right\|_{\mathcal{F}}^2}
\end{aligned}
\tag{25}
$$

However, for suitably structured dictionaries, the noise variance estimates obtained via this update rule can be extremely inaccurate [14]. Thus, in the iteration, it is recommended to use (23) and (24) for noise variance estimation.

For γ, ignoring irrelevant terms in (17), we could obtain

$$
\begin{aligned}
&\left\langle \ln \left(p(\overline{\mathbf{S}}_1 \mid \gamma) p(\overline{\mathbf{S}}_2 \mid \gamma) p(\gamma) \right) \right\rangle\\
&\propto -\sum_{i=1}^{L} \langle \overline{\mathbf{S}}_1^H(i) \Gamma^{-1} \overline{\mathbf{S}}_1(i) + \overline{\mathbf{S}}_2^H(i) \Gamma^{-1} \overline{\mathbf{S}}_2(i) \rangle\\
&\quad + 2L \ln \left(\det(\Gamma^{-1}) \right)\\
&= 2L \ln \left(\det(\Gamma^{-1}) \right) - \sum_{i=1}^{L} \operatorname{tr}\left(\Gamma^{-1}(\Sigma_{\overline{\mathbf{S}}_1} + \mu_{\overline{\mathbf{S}}_1}(i) \mu_{\overline{\mathbf{S}}_1}^H(i)) \right)\\
&\quad - \sum_{i=1}^{L} \operatorname{tr}\left(\Gamma^{-1}(\Sigma_{\overline{\mathbf{S}}_2} + \mu_{\overline{\mathbf{S}}_2}(i) \mu_{\overline{\mathbf{S}}_2}^H(i)) \right)
\end{aligned}
\tag{26}
$$

where for brevity, we have omitted the subscript $p(\overline{\mathbf{S}}_1, \overline{\mathbf{S}}_2 \mid \gamma, \beta_1, \beta_2, \mathbf{Y}_1, \mathbf{Y}_2)$ in the expectation operator and the prior distribution of γ, $\overline{\mathbf{S}}_1(i)$ and $\overline{\mathbf{S}}_2(i)$ represent the ith column of $\overline{\mathbf{S}}_1$ and $\overline{\mathbf{S}}_2$ respectively.

For convenience of calculation, we differentiate (26) with respect to $\alpha_m = \frac{1}{\gamma_m}$ instead of γ_m. Then we can have

$$\frac{\partial \langle \ln \left(p(\overline{\mathbf{S}}_1 \mid \gamma) p(\overline{\mathbf{S}}_2 \mid \gamma) p(\gamma) \right) \rangle}{\partial \alpha_m} = \frac{2L}{\alpha_m} - \Xi_{m,m} \quad (27)$$

where

$$\Xi = L(\Sigma_{\overline{\mathbf{S}}_2} + \Sigma_{\overline{\mathbf{S}}_1}) + \mu_{\overline{\mathbf{S}}_1} \mu_{\overline{\mathbf{S}}_1}^H + \mu_{\overline{\mathbf{S}}_2} \mu_{\overline{\mathbf{S}}_2}^H \quad (28)$$

and $(\cdot)_{m,m}$ represents the element at mth row and mth column of a matrix. In the above derivation, we have used the following matrix equality:

$$\frac{\partial \ln \left(\det(\Sigma^{-1}) \right)}{\alpha_m} = \mathrm{tr} \left(\Sigma \frac{\partial \Sigma^{-1}}{\partial \alpha_m} \right) \quad (29)$$

where Σ is an arbitrary matrix. Setting the derivative in (27) equal to zero, we could obtain the following update rule for γ_m

$$\gamma_m^{j+1} = \frac{\mu_{\overline{\mathbf{S}}_1}(m)^H \mu_{\overline{\mathbf{S}}_1}(m) + \mu_{\overline{\mathbf{S}}_2}(m)^H \mu_{\overline{\mathbf{S}}_2}(m)}{2L - (L\Sigma_{\overline{\mathbf{S}}_2} + L\Sigma_{\overline{\mathbf{S}}_1})_{m,m}/\gamma_m^j} \quad (30)$$

As it can be seen from (30), the update of γ_m uses the information from the average of posterior distributions of $\overline{\mathbf{S}}_1$ and $\overline{\mathbf{S}}_2$ instead of information of a single posterior distribution. As in our model, γ is the same for both stations, the average is principally equal to adding more data samples to the estimates. Therefore, the performance of our algorithm is expected to outperform traditional EM algorithm that uses data from either station.

C. COMPUTATIONAL COMPLEXITY ANALYSIS

However, the convergence of this algorithm may not be fast enough for practical applications. For the update of the posterior mean $\mu_{\overline{\mathbf{S}}_i}$, $i = 1, 2$ and posterior variance $\Sigma_{\overline{\mathbf{S}}_i}$, $i = 1, 2$, computation expense mainly comes from the matrix inversion of size $N \times N$. Thus its computational complexity is in the order of $\mathcal{O}(N^3)$. The computation of updating γ requires $2NL^2$ complex multiplications and $2(N-1)L^2$ complex additions. Following the update of γ, the update of noise variance requires $M_1 N(N + M_1) + M_2 N(N + M_2) + M_1 L(N + M_1) + M_2 L(N + M_2)$ complex multiplications and $(N - 1)M_1(N + M_1 + L) + (N - 1)M_2(N + M_2 + L) + (2L+1)M_1 + (2L+1)M_2$ complex additions. In practice, the length of the dictionary is usually much greater than the number of elements and the number of targets. Thus the computational complexity in each iteration is in the order of $\mathcal{O}(N^3)$. As N increases for higher precision of DOA estimation, the computation burden of BM-EM could be unaffordable in practice. Therefore, in the next section, we will develop a fast SBL method for DOA estimation.

D. ALGORITHM SUMMARY

The EM algorithm requires repeating the E-step and M-step until the profile of γ converges. Upon convergence, the EM algorithm would give not only the DOA estimates but also the

---

Algorithm 1 BM-EM
1) Input: $\mathbf{Y}_1$, $\mathbf{Y}_2$, Φ_1, Φ_2
2) Initialization: Set $\varepsilon = 0.001$ where ε is a small threshold value, $\gamma^0 = [1\ 1\ \cdots\ 1]^T$, $\beta_2^0 = 10$, $\beta_1^0 = 10$, $j = 0$
3) Repeat the following procedure:
   a) Calculate $\mu_{\overline{\mathbf{S}}_1}$, $\mu_{\overline{\mathbf{S}}_2}$, $\Sigma_{\overline{\mathbf{S}}_1}$ and $\Sigma_{\overline{\mathbf{S}}_2}$ by (22)
   b) Update γ^{j+1}, β_1^{j+1} and β_2^{j+1} using (30), (23) and (24) respectively
   c) Let $j = j + 1$ and continue the loop (from a) to b)) until $\frac{\|\gamma^{j+1} - \gamma^j\|_1}{\|\gamma^j\|_1} \leq \varepsilon$
4) Do the peak search of γ^{j+1} and use the dictionary matrix to obtain the angle estimation.
5) Output: θ_1, θ_2, K

---

number of sources. Thus, it does not require prior knowledge of the number of sources. The initial value of γ is usually set to be uniform in every direction of the dictionary, because no prior information of targets' possible directions is assumed. The proposed algorithm is summarized in Algorithm 1.

IV. FAST SBL METHOD

In this section, we will develop a faster DOA estimation method by maximizing the evidence function. Although this method can be much more efficient, it requires prior information about the number of targets. Similar to other DOA estimators, the number of targets can be estimated by model-order selection criteria, such as Akaike Information Criterion (AIC) and Bayesian Information Criterion (BIC) [44]–[46]. It is also possible that we introduce the model-order selection into the iteration [46], so the algorithm could work without information of the number of targets.

Instead of calculating the posterior distribution of the weights matrix $\overline{\mathbf{S}}_1$ and $\overline{\mathbf{S}}_2$, the evidence function is directly maximized to estimate the hyper-parameters. We denote this algorithm as Bi-static Multi-snapshot Sparse Bayesian Learning (BM-SBL).

According to Bayes' theorem, the evidence function could be obtained by

$$p(\mathbf{Y}_1, \mathbf{Y}_2 \mid \gamma, \beta_1, \beta_2)$$
$$= \iint p(\mathbf{Y}_1 \mid \overline{\mathbf{S}}_1, \beta_1) p(\mathbf{Y}_2 \mid \overline{\mathbf{S}}_2, \beta_2) p(\overline{\mathbf{S}}_1 \mid \gamma) p(\overline{\mathbf{S}}_2 \mid \gamma) \, d\overline{\mathbf{S}}_1 d\overline{\mathbf{S}}_2 \quad (31)$$

Substituting (8) and (9) into (31) gives

$$p(\mathbf{Y}_1, \mathbf{Y}_2 \mid \gamma, \beta_1, \beta_2) \propto \frac{e^{-\mathrm{tr}(\mathbf{Y}_1^H \Sigma_{\mathbf{Y}_1}^{-1} \mathbf{Y}_1 + \mathbf{Y}_2^H \Sigma_{\mathbf{Y}_2}^{-1} \mathbf{Y}_2)}}{\det(\Sigma_{\mathbf{Y}_1})^L \det(\Sigma_{\mathbf{Y}_2})^L} \quad (32)$$

where

$$\Sigma_{\mathbf{Y}_1} = \sigma_1^2 \mathbf{I}_{M1} + \Phi_1 \Gamma \Phi_1^H, \ \Sigma_{\mathbf{Y}_2} = \sigma_2^2 \mathbf{I}_{M2} + \Phi_2 \Gamma \Phi_2^H \quad (33)$$

With (32), the hyper-parameters are estimated by

$$(\gamma^\star, \beta_1^\star, \beta_2^\star) = \underset{\gamma, \beta_1, \beta_2}{\arg\max} \ln(p(\mathbf{Y}_1, \mathbf{Y}_2 \mid \gamma, \beta_1, \beta_2)) \quad (34)$$

The maximization is carried out by alternatively updating the hyper-parameters.

A. UPDATE FOR γ

In this subsection, we will address the update for γ. Differentiating (34) with respect to γ_m gives us

$$
\frac{\partial \ln p(\mathbf{Y}_1, \mathbf{Y}_2 \mid \gamma, \beta_1, \beta_2)}{\partial \gamma_m}
$$
$$
= \left\| \mathbf{Y}_1^H \Sigma_{\mathbf{Y}_1}^{-1} \phi_{1m} \right\|_2^2 + \left\| \mathbf{Y}_2^H \Sigma_{\mathbf{Y}_2}^{-1} \phi_{2m} \right\|_2^2 - L \phi_{1m}^H \Sigma_{\mathbf{Y}_1}^{-1} \phi_{1m}
$$
$$
- L \phi_{2m}^H \Sigma_{\mathbf{Y}_2}^{-1} \phi_{2m} \qquad (35)
$$

where ϕ_{1m} and ϕ_{2m} are the mth column of Φ_1 and Φ_2 respectively. In derivation of (35), we have used the following matrix equality:

$$
\frac{\partial \Sigma^{-1}}{\partial \gamma_m} = -\Sigma^{-1} \frac{\Sigma}{\gamma_m} \Sigma^{-1} \qquad (36)
$$

where Σ is an arbitrary matrix.

Using fix-point method, we introduce factors into (35) to obtain an iterative update equation for γ_m. Thus we rewrite (35) as

$$
\frac{\partial \ln p(\mathbf{Y}_1, \mathbf{Y}_2 \mid \gamma, \beta_1, \beta_2)}{\partial \gamma_m}
$$
$$
= \left(\frac{\gamma_m^j}{\gamma_m^{j+1}} \right)^2 \left\| \mathbf{Y}_1^H \Sigma_{\mathbf{Y}_1}^{-1} \phi_{1m} \right\|_2^2 - L \phi_{1m}^H \Sigma_{\mathbf{Y}_1}^{-1} \phi_{1m}
$$
$$
+ \left(\frac{\gamma_m^j}{\gamma_m^{j+1}} \right)^2 \left\| \mathbf{Y}_2^H \Sigma_{\mathbf{Y}_2}^{-1} \phi_{2m} \right\|_2^2 - L \phi_{2m}^H \Sigma_{\mathbf{Y}_2}^{-1} \phi_{2m} \qquad (37)
$$

Setting (37) to zero, we can get the update rule for γ_m as

$$
\gamma_m^{j+1} = \gamma_m^j \sqrt{\frac{\left\| \mathbf{Y}_1^H \Sigma_{\mathbf{Y}_1}^{-1} \phi_{1m} \right\|_2^2 + \left\| \mathbf{Y}_2^H \Sigma_{\mathbf{Y}_2}^{-1} \phi_{2m} \right\|_2^2}{L \phi_{1m}^H \Sigma_{\mathbf{Y}_1}^{-1} \phi_{1m} + L \phi_{2m}^H \Sigma_{\mathbf{Y}_2}^{-1} \phi_{2m}}} \qquad (38)
$$

Note that from (5), we have

$$
\left\| \mathbf{Y}_i^H \Sigma_{\mathbf{Y}_i}^{-1} \phi_{im} \right\|_2^2 = L \phi_{im}^H \Sigma_{\mathbf{Y}_i}^{-1} \mathbf{R}_i \Sigma_{\mathbf{Y}_i}^{-1} \phi_{im}, \; i = 1, 2 \qquad (39)
$$

Therefore, once $\Sigma_{\mathbf{Y}_i} = \mathbf{R}_i$, we will have $\gamma_m^j = \gamma_m^{j+1}$. Now we can see that the update of γ is principally an iterative procedure of fitting the covariance matrix. At the optimal point, we have the following equation [47]

$$
\Phi_{i\mathcal{M}}^H (\mathbf{R}_i - \Sigma_{\mathbf{Y}_i}) \Phi_{i\mathcal{M}} = \mathbf{0}, \; i = 1, 2 \qquad (40)
$$

where $\Phi_{1\mathcal{M}}$ and $\Phi_{2\mathcal{M}}$ are composed of columns from Φ_1 and Φ_2 that correspond to the target directions. Since $\mathbf{R}_1$ and $\mathbf{R}_2$ are usually positive definite, we can replace $\Sigma_{\mathbf{Y}_1}^{-1}$ and $\Sigma_{\mathbf{Y}_2}^{-1}$ in (38) with $\mathbf{R}_1^{-1}$ and $\mathbf{R}_2^{-1}$ respectively [47] and we can rewrite the update rule as

$$
\gamma_m^{j+1} = \gamma_m^j \sqrt{\frac{\left\| \mathbf{Y}_1^H \Sigma_{\mathbf{Y}_1}^{-1} \phi_{1m} \right\|_2^2 + \left\| \mathbf{Y}_2^H \Sigma_{\mathbf{Y}_2}^{-1} \phi_{2m} \right\|_2^2}{L \phi_{1m}^H \mathbf{R}_1^{-1} \phi_{1m} + L \phi_{2m}^H \mathbf{R}_2^{-1} \phi_{2m}}} \qquad (41)
$$

Such replacement can reduce the computation expense at each iteration.

In [47], a similar algorithm for only one station was proposed where the update rule for γ_m is

$$
\gamma_m^{j+1} = \frac{\gamma_m^j}{\sqrt{L}} \left\| \mathbf{Y}_1^H \Sigma_{\mathbf{Y}_1}^{-1} \phi_{1m} \right\|_2^2 \Big/ \sqrt{\phi_{1m}^H \mathbf{R}_1^{-1} \phi_{1m}} \qquad (42)
$$

It can be seen that (41) is not a linear combination of the update rule in (42) for a single station. The convergence of the proposed algorithm using (41) not only depends on the data variance fitting of station 1 but also the data variance fitting of station 2. Thus more data samples are used for estimation. Using (41) to update γ_m is more robust to small perturbations in the proximity of the optimal value.

Guarantees for global convergence is hard to prove rigorously. In [47], the proof of convergence of (42) was not provided. As the formulated problem falls into the category of multi-task compressive sensing, it has been proved that the global minimum of the joint reconstruction process as in BM-SBL coincides with the true solution with probability 1 in the noiseless case [48]. In this paper, we give the local convergence of BM-SBL:

Theorem 2: $\exists$ a set $\mathbb{K} = \left\{ \gamma \mid \delta \geq \gamma_m - \gamma_m^* \geq 0 \right\}$ such that if the initial point of the iteration $\gamma^0 \in \mathbb{K}$, the algorithm would always converge to the true value γ^*.

The proof of the above theorem is provided in Appendix B.

B. ESTIMATION OF K AND UPDATE FOR σ_1^2, σ_2^2

Before jumping into the estimation of noise variance, we need to determine the number of targets first. Following the guidelines in [46], one can easily get the estimate of K as

$$
\hat{K} = \arg\max_P \left\{ M_i L \ln \left(\frac{\text{tr} \left((\mathbf{I} - \mathbf{P}_i) \mathbf{R}_i \right)}{M_i - P} \right) - LP + \kappa \right\},
$$
$$
i = 1 \text{ or } 2 \qquad (43)
$$

where P is the model order, $\kappa = \frac{(2PL+1)\ln(L)}{2}$ and

$$
\mathbf{P}_1 = \Phi_{1\mathcal{M}} (\Phi_{1\mathcal{M}}^H \Phi_{1\mathcal{M}})^{-1} \Phi_{1\mathcal{M}}^H
$$
$$
\mathbf{P}_2 = \Phi_{2\mathcal{M}} (\Phi_{2\mathcal{M}}^H \Phi_{2\mathcal{M}})^{-1} \Phi_{2\mathcal{M}}^H \qquad (44)
$$

are the subspace projection matrices. Here $\Phi_{1\mathcal{M}}$ and $\Phi_{2\mathcal{M}}$ are composed of columns from Φ_1 and Φ_2 that correspond to the directions of P largest peaks in γ.

Getting a good estimate of noise variance is important for fast convergence of the SBL methods. As it can be seen from the last section, the estimation of noise only depends on either $\mathbf{Y}_1$ or $\mathbf{Y}_2$. Therefore, we can follow the same procedure as in [47] to get the update rule as

$$
\sigma_1^2 = \frac{\text{tr} \left((\mathbf{I} - \mathbf{P}_1) \mathbf{R}_1 \right)}{M_1 - K}, \; \sigma_2^2 = \frac{\text{tr} \left((\mathbf{I} - \mathbf{P}_2) \mathbf{R}_2 \right)}{M_2 - K} \qquad (45)
$$

The above update rule is an outcome of (40). Note that $\mathbf{P}_1$ and $\mathbf{P}_2$ may change at every iteration until the algorithm converges. If the columns in $\Phi_{1\mathcal{M}}$ and $\Phi_{2\mathcal{M}}$ correspond to the true target directions, the noise estimate in (45)

is unbiased, consistent and asymptotically efficient as it approaches the Cramer-Rao Lower Bound (CRLB) with $L \to \infty$ [47]. But if the columns in $\Phi_{1\mathcal{M}}$ and $\Phi_{2\mathcal{M}}$ correspond to the false directions, (45) will always over-estimate the noise power because the signal power is smeared into noise subspace.

C. COMPUTATIONAL COMPLEXITY ANALYSIS

In each iteration, the computation expense of updating γ is mostly on calculation of the numerator, as the denominator does not change with iteration and can be calculated in advance. The computation of $\Sigma_{\mathbf{Y}_1}^{-1}$ and $\Sigma_{\mathbf{Y}_2}^{-1}$ is in the order of $\mathcal{O}(M_1^3)$ and $\mathcal{O}(M_2^3)$ respectively and the update of γ requires about $N((L + 2M_1 + 1)M_1 + (L + 2M_2 + 1)M_2 + 2L)$ times complex multiplications and $N(M_1 - 1)(2M_1 + L + 1) + N(M_2 - 1)(2M_2 + L + 1)$ complex additions. For the update of noise variance, determining the number of targets needs to be done in advance. Afterwards, the update of noise variance can be obtained directly from the maximum of the object function in (43). If simple traversal search is used for finding the solution of (43), the computation requires $\sum_{P=1}^{\eta} 2(M_1 + M_2 + P)P^2 + PM_1^2 + PM_2^2 + M_1^3 + M_2^3$ complex multiplications and $\sum_{P=1}^{\eta}(M_1 - 1)(M_1^2 + P^2 + 2) + (P - 1)(M_1P + M_1^2) + (M_2 - 1)(M_2^2 + P^2 + 2) + (P - 1)(M_2P + M_2^2) + 2P^3$ complex additions where η is the maximum number of P. Generally η is much less than the minimum of M_1 and M_2. Since the number of elements and the number of targets are much less than N, the computation in each iteration of Algorithm 2 is much less than BM-EM.

D. ALGORITHM SUMMARY

The algorithm proceeds by repetitively and alternatively update γ and σ_1^2, σ_2^2 until $\frac{\|\gamma^{j+1} - \gamma^j\|_1}{\|\gamma^j\|_1} \le \varepsilon$. Firstly the update of γ is done using (41), then the first K highest peaks are picked out to form $\Phi_{1\mathcal{M}}$ and $\Phi_{2\mathcal{M}}$. Afterwards, σ_1^2 and σ_2^2 are updated by (45). The algorithm proposed in this section estimate the targets' DOA by iterative fitting the data covariance. Therefore, the better estimation of $\mathbf{R}_1$ and $\mathbf{R}_2$ we have, the better estimation of DOA we can achieve. Note that the update of noise variance in (45) may converge very fast to its optimal point if $M_1 \gg K$ and $M_2 \gg K$ because the initial estimate may be already close to the optima, which would accelerate the convergence of our algorithm. The algorithm is summarized in Algorithm 2.

V. SIMULATION RESULTS

In this section, we conduct mathematical simulation to demonstrate the convergent property and estimation performance of the proposed algorithms. We compare our methods with the other conventional DOA estimation methods, such as MUSIC, Empirical Multi-snapshot Sparse Bayesian Learning (EM-SBL) [14], original one-station EM (O-EM) [42], [49], and Multi-snapshot Sparse Bayesian Learning (M-SBL) [47].

Algorithm 2 BM-SBL

1) Input: $\mathbf{Y}_1, \mathbf{Y}_2, \Phi_1, \Phi_2$
2) Initialization: Set $\varepsilon = 0.001$ where ε is a small threshold value, $\gamma^0 = [1 \ 1 \ \cdots \ 1]^T$, $\beta_2^0 = 10$, $\beta_1^0 = 10$, $j = 0$. Estimate $\mathbf{R}_1$ and $\mathbf{R}_2$ by (5), calculate $\mathbf{R}_1^{-1}$ and $\mathbf{R}_2^{-1}$
3) Repeat the following procedure:
   a) Calculate $\Sigma_{\mathbf{Y}_1}$ and $\Sigma_{\mathbf{Y}_2}$ using (33) and calculate $\Sigma_{\mathbf{Y}_1}^{-1}$, $\Sigma_{\mathbf{Y}_2}^{-1}$ accordingly
   b) Update γ^{j+1} using (41)
   c) Determine K using (43)
   d) $\mathcal{M} = \{m \in \mathbb{N} | K$ largest peaks in $\gamma\}$, build $\Phi_{i\mathcal{M}}$, $i = 1, 2$ accordingly
   e) Update $(\sigma_1^2)^{j+1}$ and $(\sigma_2^2)^{j+1}$ using (45)
   f) Let $j = j + 1$ and continue the loop (from a) to d)) until $\frac{\|\gamma^{j+1} - \gamma^j\|_1}{\|\gamma^j\|_1} \le \varepsilon$
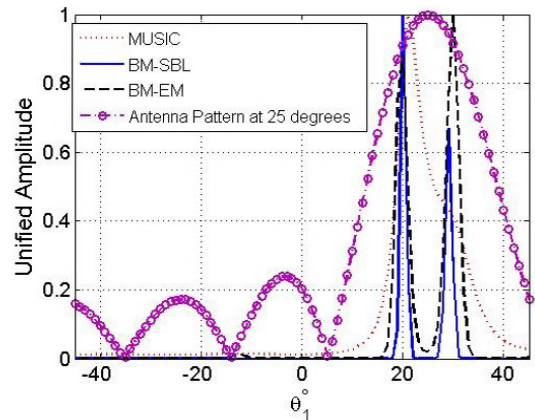4) Output: θ_1, θ_2

FIGURE 2. Spectral of the proposed algorithms.

These conventional methods only utilize data from station with higher SNR. For well-separated targets, all sparsity-inducing methods as well as MUSIC would provide similar DOA estimation performance, they differ, however, when two of the targets are closely located.

We consider two stations both equipped with linear array of six elements. The elements are uniformly spaced by half of the wavelength of radar. In this section, the simulation is conducted based on two different scenarios. In the first scenario, the distance between station 1 and the cross point equals the distance between station 2 and the cross point, i.e. $L_1 = L_2$ and the range of station 1 and of station 2 is the same and is equal to L_1, i.e. $R_1 = R_2 = L_1$. In this special case, the dictionary Φ_2 is merely a mirror image of Φ_1. Thus, the grids of two dictionaries are both uniformly sampled in space and we have $\theta_1 = -\theta_2$. In the second scenario, we also assume that $L_1 = L_2$, but $R_1 = 2L_1$, $R_2 = 1.8L_1$. In this scenario, the grids of dictionary Φ_1 are still uniformly sampled but the grids of Φ_2 are calculated according to (2).
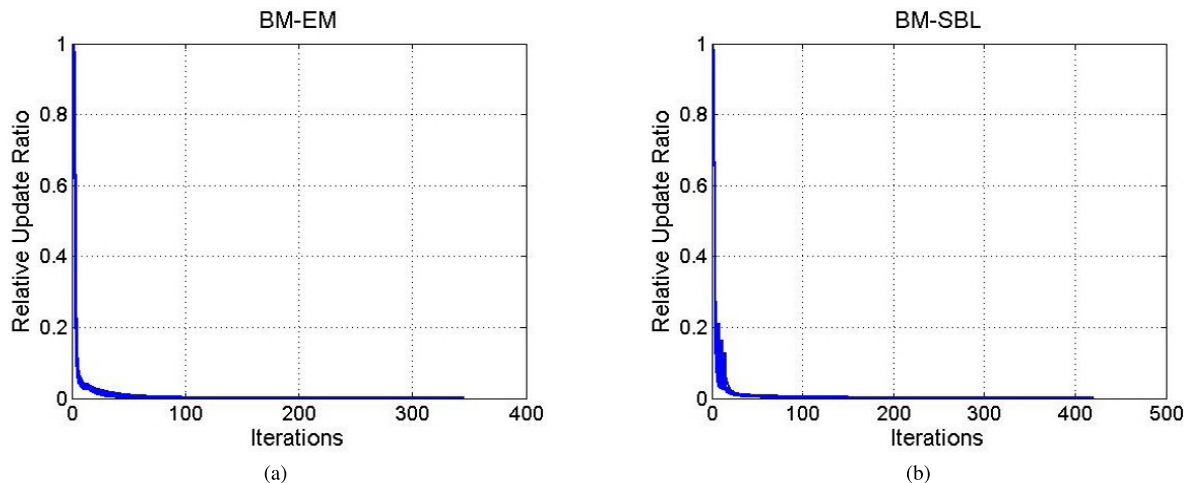
FIGURE 3. Relative update ratio of γ, (a) BM-EM; (b) BM-SBL.

A. SPECTRA AND CONVERGENT ANALYSIS OF THE PROPOSED ALGORITHMS

In this subsection, simulation is conducted to analyze spectra and convergent property of the proposed algorithms. The simulation is based on scenario 1. The dictionary of station 1 spans from $-45°$ to $45°$ at an interval of $1°$. Consider that two targets are incident upon the arrays. The incidental angle of the first target with respect to station 1 is $20°$ and the incidental angle of the second target with respect to station 1 is $30°$. Assume that the SNR of station 2 is 0dB and the SNR of station 1 is 6dB lower than station 2. Each station collects 50 samples for estimation. The spectra of the proposed algorithms are shown in Fig. 2 where the spectrum of MUSIC is used as a comparison. The beam pattern of array 1 at the direction of $25°$ is also plotted in Fig 2. From Fig. 2, it can be seen that the proposed algorithms can obtain precise estimation of two closely spaced targets (within the 3dB beam width of the main lobe) while the MUSIC algorithm fails to distinguish the two targets. It can also be observed that the peak width of BM-SBL is narrower than BM-EM.

To analyze the convergent property of the proposed algorithms, we take the relative update ratio $\frac{\|\gamma^{j+1}-\gamma^j\|_1}{\|\gamma^j\|_1}$ as a measure of convergence. The relative update ratio can tell the rate of convergence and whether fluctuation occurred during iterations. In the simulation, we cap the number of iterations to be 500 in BM-EM and BM-SBL. The results of 10 Monte Carlo simulations are plotted in Fig. 3. From the results, we can see that the relative update ratio of γ drops rapidly at the beginning and barely changes after about 300 iterations for both algorithms. However, in BM-SBL the relative update ratio undergoes a small bump after the rapid drop which is the result of fitting the covariance matrix. As the eigenvalues of Σ_{Y_1} and Σ_{Y_2} approach that of R_1 and R_2 respectively, a sudden turn of direction would generally happen once the convergent sequences of eigenvalues cross the eigenvalues of R_1 and R_2.

The ratio σ_1^2/σ_{1T}^2 is used to evaluate the convergence of noise variance estimation, where σ_{1T}^2 is the true value of the noise variance in station 1. The results are plotted in Fig. 4. From the results, it can be seen that the BM-EM tends to underestimate the noise variance while the BM-SBL tends to produce rather precise estimates at the beginning of the iteration. As can be seen, the estimate of noise variance for BM-SBL is always higher than its true value at the beginning of the iteration, which is consistent with the analysis in Section IV.

B. DOA ESTIMATION PERFORMANCE

In this subsection, we will compare the DOA estimation performance of the proposed algorithms with conventional methods. Two targets are assumed with $\theta_{11} = 20°$ and $\theta_{12} = 30°$ respectively. As shown in Fig. 2, when the two targets are such closely placed, the traditional MUSIC algorithm would not be able to distinguish between them. Thus, the comparison does not include MUSIC. We set the SNR in station 1 3dB higher than the SNR in station 2. The simulation is conducted based on the two different scenarios mentioned above.

In the first scenario, each method collects 50 independent snapshots for estimation and 100 Monte Carlo simulations are conducted to evaluate the performance. The conventional methods, i.e. EM-SBL, O-EM and M-SBL, only utilize the data from station 1. Fig. 5 shows the RMSE of different methods for different SNR of station 2. It can be seen from the results that in this scenario, the proposed algorithms, i.e. BM-EM and BM-SBL both outperform the conventional methods at all different SNR which is due to the incorporation of the data samples from station 2. Furthermore, the BM-SBL has a slight advantage over BM-EM in RMSE, especially when the SNR is low, which probably results from the usage of prior information about the number of targets. For the same reason, M-SBL outperforms EM-SBL and O-EM in all cases. The EM-SBL and O-EM fail to produce precise estimation of targets DOA when the SNR drops below 0dB. The advantage
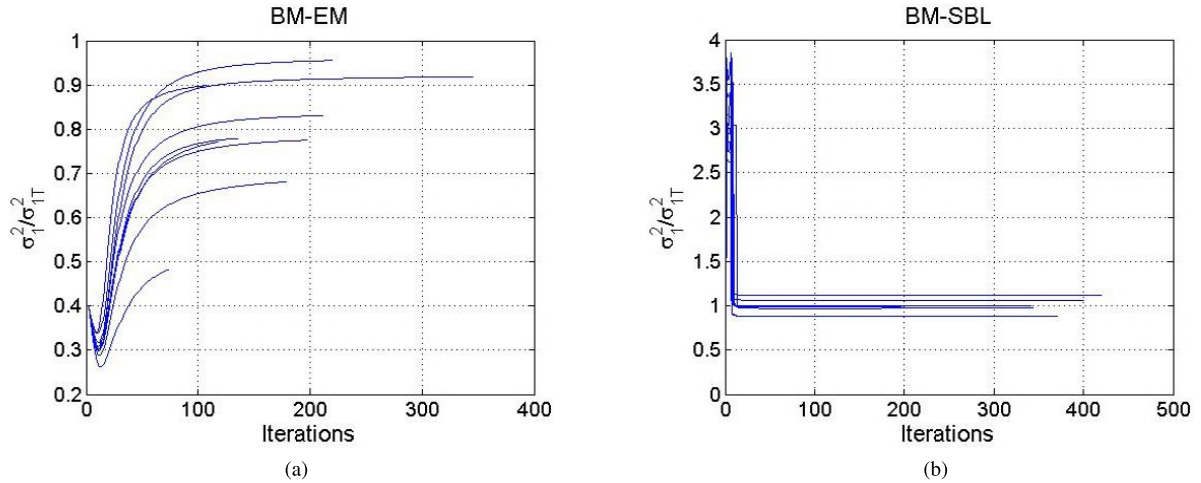
FIGURE 4. Convergence of noise variance σ_1^2, (a) BM-EM; (b) BM-SBL.
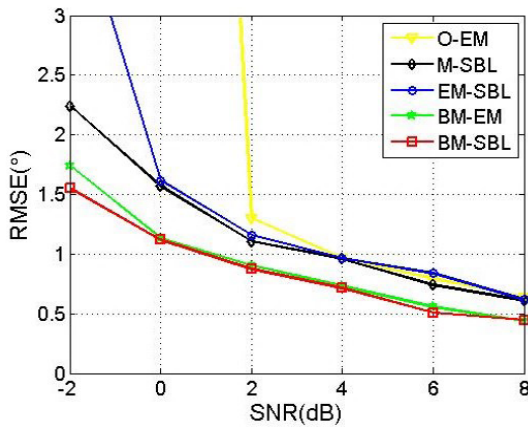

FIGURE 5. RMSE of different methods versus SNR in scenario 1.
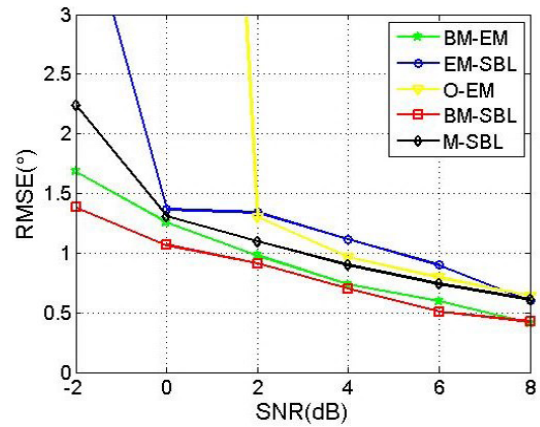

FIGURE 6. RMSE of different methods versus SNR in scenario 2.

of the proposed algorithms is more obvious in the case of low SNR. Thus it can be concluded that in this scenario, the joint estimation obtained via the proposed methods can achieve better performance than the conventional SBL methods only using data from one station. Fig. 6 shows the RMSE of different methods versus the SNR of station 2 in scenario 2. Again, each method uses 50 snapshots for estimation and the RMSE is calculated based on 100 Monte Carlo simulations. It can be seen that in this scenario, the proposed algorithms still outperform the all the other conventional SBL methods, especially at lower SNR.

Fig. 7 shows the how performance of different methods changes with different number of snapshots in scenario 1. In the scenario, it is still assumed that two targets are incident from the direction $\theta_{11} = 20°$ and the direction $\theta_{12} = 30°$ respectively. The SNR of both stations are set to be 4dB. The RMSE of each method is calculated based on 100 Monte Carlo simulations. It can be seen that the performance of all the sparsity-inducing techniques improves with increasing number of snapshots. The proposed algorithms outperform the other conventional methods in all situations. It can also
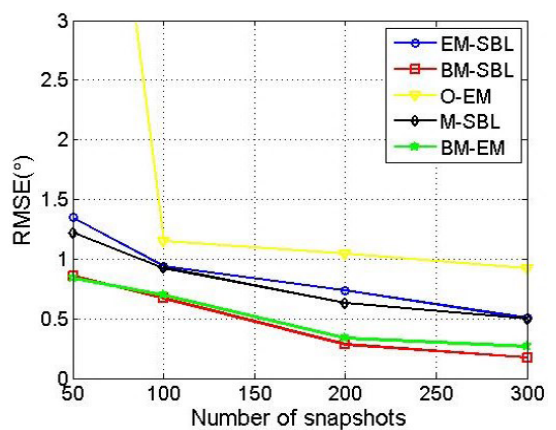

FIGURE 7. RMSE of different methods versus number of snapshots in scenario 1.

be observed that when the number of snapshots grows larger, BM-SBL has a slight advantage in RMSE over BM-EM.

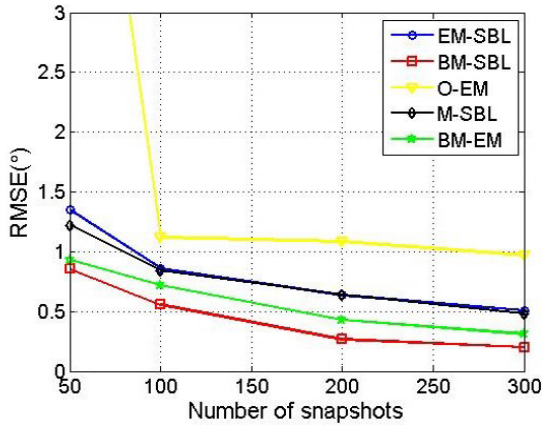Fig. 8 shows the RMSE of different methods versus number of samples in scenario 2. In scenario 2, the dictionary

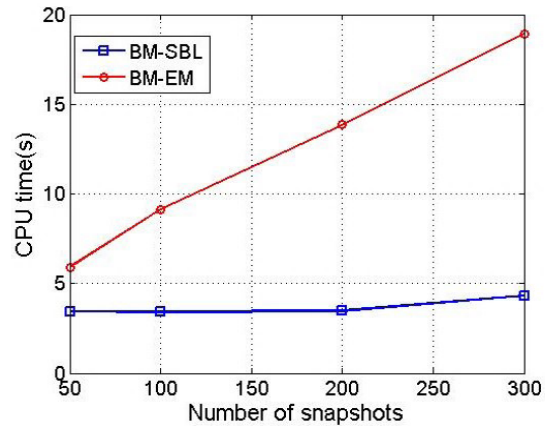**FIGURE 8.** RMSE of different methods versus number of snapshots in scenario 2.

FIGURE 9. RMSE of different methods versus separated angle between targets in scenario 1.

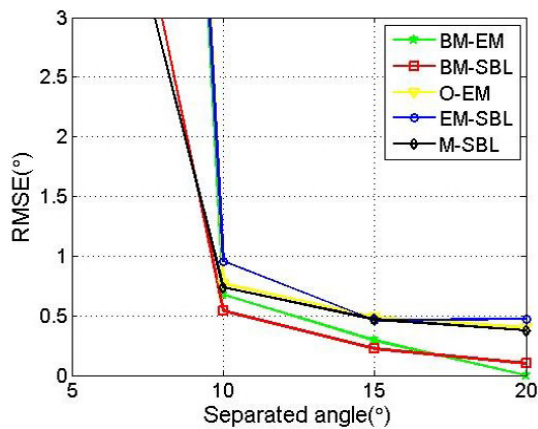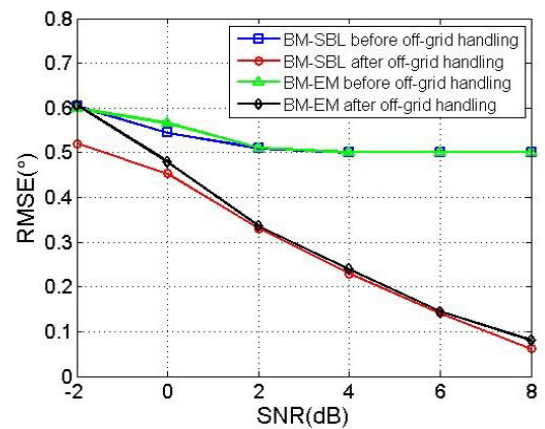**FIGURE 10.** Computation time of the proposed methods versus number of snapshots in scenario 1.

FIGURE 11. RMSE of the proposed algorithm versus SNR before and after the off-grid handling.

FIGURE 12. Computation time of the proposed methods versus number of snapshots before and after the off-grid handling.

Φ_2 is no longer uniformly sampled. All the other simulation parameters remain the same as in scenario 1. From the results, it can also be found that the proposed algorithms outperform the other conventional methods and the BM-SBL tends to perform better than BM-EM in the case of large number of samples.

Fig. 9 presents the performance of different methods at different cases where the two targets are separated by different angles. In the simulation, the first target is fixed at $0°$, while the angle of the other target changes from $5°$ to $20°$. It is found that all the SBL methods are not able to tell the two targets separated by less than $5°$ and when the targets are separated by more than $10°$, the SBL methods can produce relatively precise estimates. It is also seen that the larger the separated angle is, the lower RMSE the SBL methods can offer. The proposed algorithms outperform the conventional methods in all situations.

The computation time of BM-EM and BM-SBL is compared in Fig. 10. It can be seen that with more snapshots, the algorithms require more time for calculation. Furthermore, BM-SBL is clearly more computational efficient than BM-EM, especially in the cases of large snapshots, which support the analysis given in Section IV.

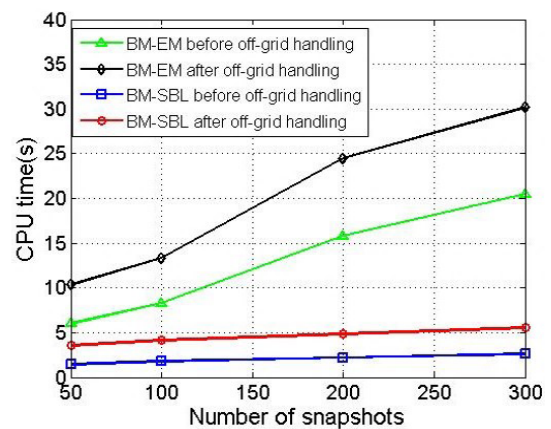DOA estimation performance with and without the grid refining strategy [15] is compared in Fig. 11. In the simulation, two targets were assumed. The incidental angles with respect to station 1 were $10°$ and $-10.5°$ respectively. 100 snapshots were used for the estimation. The SNR

changed from -2dB to 8dB. In the off-grid handling, the grids of the refined dictionary matrix span from $\min(\hat{\theta}) - 5°$ to $\max(\hat{\theta}) + 5°$ with the interval being $0.5°$. Here $\hat{\theta}$ is the DOA estimates from the last estimation using coarse grids. Such choice of grids was made based on the last estimates of targets' DOA. It ensured that all the DOA of targets were covered in the refined grids. It can be seen from Fig. 11 that the off-grid handling can significantly improve the performance of DOA estimation. Without the off-grid handling, the RMSE could not go lower than $0.5°$. The computational complexity of the proposed method before and after the off-grid handling was compared in Fig. 12. It can be seen that with snapshots increasing, the computation complexity of BM-SBL increases slower than that of BM-EM. The off-grid handling almost doubles the CPU time of the case without off-grid handling. In all, the off-grid handling is able to deal with the off-grid targets, however at the expense of much more computational resources.

VI. CONCLUSION

In this paper, we proposed a novel DOA estimation method for bi-static passive radar under the framework of sparse Bayesian learning, which successfully combined the measurements from both stations to achieve improved estimates. Theoretical results showed that the bi-static system could help enhance the uniqueness of the reconstructed solution. Two algorithms were proposed for this purpose. The MAP estimator was firstly derived using EM technique. To reduce the computation expenses, a fast SBL method named BM-SBL was then developed by using the fix-point method to maximize the evidence. Theoretical derivation proved that once the initial point of iteration started in a given set around the true value, the BM-SBL estimates would always converge to the true value. Simulation results demonstrate the advantage of the proposed algorithms against the conventional SBL methods only using data from one station.

APPENDIX A
PROOF OF THEOREM 1

Proof: The proof of theorem 1 follows the basic guideline of proving Theorem 1 in [17], [21], [35] for single-task compressive sensing. As the formulated problem in this paper is a multi-task compressive sensing, the derivation differs a little.

Let us assume that $M_1 > M_2$ and there exists another solution of $\overline{\mathbf{S}}_1$ with diversity $r < M_1 - p + 1$. Denote such solution as $\overline{\mathbf{S}}_1{}'$. Then we have

$$\Phi_1 \overline{\mathbf{S}}_1 = \Phi_1 \overline{\mathbf{S}}_1{}' \tag{46}$$

Denote the p columns in Φ_1 that correspond to the non-zero rows in $\overline{\mathbf{S}}_1$ as Φ_1^p and the sub-matrix that is formed by the non-zero rows of $\overline{\mathbf{S}}_1$ as $\mathbf{X}_1$. Denote the r columns in Φ_1 that correspond to the non-zero rows in $\overline{\mathbf{S}}_1{}'$ as Φ_1^r and the sub-matrix that is formed by the non-zero rows of $\overline{\mathbf{S}}_1{}'$ as $\mathbf{X}_2$.

Thus, following the assumption, one can get

$$(\Phi_1^p \ \Phi_1^r) \begin{pmatrix} \mathbf{X}_1 \\ -\mathbf{X}_2 \end{pmatrix} = \mathbf{0} \tag{47}$$

Since $p + r < m_1$, the columns in the matrix $(\Phi_1^p \ \Phi_1^r)$ are linearly independent. Therefore, $\mathbf{X}_1$ and $\mathbf{X}_2$ must be zero matrix for (47) to be satisfied, which clearly contradicts the original assumption. The above derivation concludes that there can be no other solution of $\overline{\mathbf{S}}_1$ with diversity $r < m_1 - p + 1$. As $p < \frac{m}{2}$, it can be given that $r > p$ which means that the original solution is the sparsest among all that satisfy (7). The same conclusion can be derived if $m_2 > m_1$ and hence, theorem 1 is proved. ∎

APPENDIX B
PROOF OF THEOREM 2

Proof: In order to access the convergence of sequence γ_m, we firstly prove the local convergence of the sequence γ_m^2. From (41), we have

$$(\gamma_m^{j+1})^2 = (\gamma_m^j)^2 \frac{\left\| \mathbf{Y}_1^H \Sigma_{\mathbf{Y}_1}^{-1} \phi_{1m} \right\|_2^2 + \left\| \mathbf{Y}_2^H \Sigma_{\mathbf{Y}_2}^{-1} \phi_{2m} \right\|_2^2}{L\phi_{1m}^H \mathbf{R}_1^{-1} \phi_{1m} + L\phi_{2m}^H \mathbf{R}_2^{-1} \phi_{2m}} \tag{48}$$

Taking differentiation of (48) over γ_m^2 gives:

$$\frac{\partial (\gamma_m^{j+1})^2}{\partial (\gamma_m^j)^2} = \frac{\left\| \mathbf{Y}_1^H \Sigma_{\mathbf{Y}_1}^{-1} \phi_{1m} \right\|_2^2 + \left\| \mathbf{Y}_2^H \Sigma_{\mathbf{Y}_2}^{-1} \phi_{2m} \right\|_2^2}{L\phi_{1m}^H \mathbf{R}_1^{-1} \phi_{1m} + L\phi_{2m}^H \mathbf{R}_2^{-1} \phi_{2m}}$$
$$+ \frac{\frac{\partial \left\| \mathbf{Y}_1^H \Sigma_{\mathbf{Y}_1}^{-1} \phi_{1m} \right\|_2^2}{\partial (\gamma_m^j)^2} (\gamma_m^j)^2 + \frac{\partial \left\| \mathbf{Y}_2^H \Sigma_{\mathbf{Y}_2}^{-1} \phi_{2m} \right\|_2^2}{\partial (\gamma_m^j)^2} (\gamma_m^j)^2}{L\phi_{1m}^H \mathbf{R}_1^{-1} \phi_{1m} + L\phi_{2m}^H \mathbf{R}_2^{-1} \phi_{2m}} \tag{49}$$

The complex derivative operator is defined in [50]

$$\frac{\partial f}{\partial \mathbf{x}} = \frac{\partial f}{\text{Re}(\mathbf{x})} - j \frac{\partial f}{\text{Im}(\mathbf{x})} \tag{50}$$

where f is an arbitrary real function and $\mathbf{x}$ is a complex vector, $\text{Re}(\cdot)$ and $\text{Im}(\cdot)$ represent the real part and imaginary part of a complex matrix respectively.

Using the complex derivative operator and the chain rule of differentiation, we have

$$\frac{\partial \left\| \mathbf{Y}_1^H \Sigma_{\mathbf{Y}_1}^{-1} \phi_{1m} \right\|_2^2}{\partial (\gamma_m^j)^2}$$
$$= \left(\frac{\partial \left\| \mathbf{Y}_1^H \Sigma_{\mathbf{Y}_1}^{-1} \phi_{1m} \right\|_2^2}{\partial (\mathbf{Y}_1^H \Sigma_{\mathbf{Y}_1}^{-1} \phi_{1m})} \right)^T \frac{\partial (\mathbf{Y}_1^H \Sigma_{\mathbf{Y}_1}^{-1} \phi_{1m})}{\partial (\gamma_m^j)^2}$$
$$= 2(\mathbf{Y}_1^H \Sigma_{\mathbf{Y}_1}^{-1} \phi_{1m})^H \left(-\mathbf{Y}_1^H \Sigma_{\mathbf{Y}_1}^{-1} \phi_{1m} \frac{1}{2\gamma_m^j} \phi_{1m}^H \Sigma_{\mathbf{Y}_1}^{-1} \phi_{1m} \right)$$
$$= -\frac{\phi_{1m}^H \Sigma_{\mathbf{Y}_1}^{-1} \phi_{1m}}{\gamma_m^j} \left\| \mathbf{Y}_1^H \Sigma_{\mathbf{Y}_1}^{-1} \phi_{1m} \right\|_2^2 \tag{51}$$

where in the above derivation, we have used

$$\frac{\partial(\Sigma_{\mathbf{Y}_1}^{-1})}{\partial(\gamma_m^j)^2} = -\Sigma_{\mathbf{Y}_1}^{-1}\frac{\partial(\Sigma_{\mathbf{Y}_1})}{\partial(\gamma_m^j)^2}\Sigma_{\mathbf{Y}_1}^{-1}$$

$$= -\Sigma_{\mathbf{Y}_1}^{-1}\phi_{1m}\frac{1}{2\gamma_m^j}\phi_{1m}^H\Sigma_{\mathbf{Y}_1}^{-1} \quad (52)$$

Similarly, one can easily get

$$\frac{\partial\left\|\mathbf{Y}_2^H\Sigma_{\mathbf{Y}_2}^{-1}\phi_{2m}\right\|_2^2}{\partial(\gamma_m^j)^2} = -\frac{\phi_{2m}^H\Sigma_{\mathbf{Y}_2}^{-1}\phi_{2m}}{\gamma_m^j}\left\|\mathbf{Y}_2^H\Sigma_{\mathbf{Y}_2}^{-1}\phi_{2m}\right\|_2^2 \quad (53)$$

Substituting (51) and (53) into (49) gives that

$$\frac{\partial(\gamma_m^{j+1})^2}{\partial(\gamma_m^j)^2} = \frac{\left\|\mathbf{Y}_1^H\Sigma_{\mathbf{Y}_1}^{-1}\phi_{1m}\right\|_2^2(1 - \gamma_m\phi_{1m}^H\Sigma_{\mathbf{Y}_1}^{-1}\phi_{1m})}{L\phi_{1m}^H\mathbf{R}_1^{-1}\phi_{1m} + L\phi_{2m}^H\mathbf{R}_2^{-1}\phi_{2m}}$$

$$+ \frac{\left\|\mathbf{Y}_2^H\Sigma_{\mathbf{Y}_2}^{-1}\phi_{2m}\right\|_2^2(1 - \gamma_m\phi_{2m}^H\Sigma_{\mathbf{Y}_2}^{-1}\phi_{2m})}{L\phi_{1m}^H\mathbf{R}_1^{-1}\phi_{1m} + L\phi_{2m}^H\mathbf{R}_2^{-1}\phi_{2m}} \quad (54)$$

In the following derivation, the lemma below is used:

Lemma 1: Define a real function $g(\gamma_m) = \gamma_m\phi_{im}^H\Sigma_{\mathbf{Y}_i}^{-1}\phi_{im}$, $i = 1$ or 2 on the domain $\mathbb{D} = \mathbb{R}^+ \cup \{0\}$, then $\sup(g(\gamma_m)) \leq 1$.

With the Lemma, it can be seen that $\frac{\partial(\gamma_m^{j+1})^2}{\partial(\gamma_m^j)^2} \geq 0$. Define another function $h_m(\gamma) = \frac{\partial(\gamma_m^{j+1})^2}{\partial(\gamma_m^j)^2}$. Such function is a multivariate function. The derivative of $h_m(\gamma)$ over γ_m is

$$\frac{\partial h(\gamma_m)}{\partial\gamma_m}$$

$$= \frac{-3\left\|\mathbf{Y}_1^H\Sigma_{\mathbf{Y}_1}^{-1}\phi_{1m}\right\|_2^2(1 - \gamma_m\phi_{1m}^H\Sigma_{\mathbf{Y}_1}^{-1}\phi_{1m})\phi_{1m}^H\Sigma_{\mathbf{Y}_1}^{-1}\phi_{1m}}{L\phi_{1m}^H\mathbf{R}_1^{-1}\phi_{1m} + L\phi_{2m}^H\mathbf{R}_2^{-1}\phi_{2m}}$$

$$+ \frac{-3\left\|\mathbf{Y}_2^H\Sigma_{\mathbf{Y}_2}^{-1}\phi_{2m}\right\|_2^2(1 - \gamma_m\phi_{2m}^H\Sigma_{\mathbf{Y}_2}^{-1}\phi_{2m})\phi_{2m}^H\Sigma_{\mathbf{Y}_2}^{-1}\phi_{2m}}{L\phi_{1m}^H\mathbf{R}_1^{-1}\phi_{1m} + L\phi_{2m}^H\mathbf{R}_2^{-1}\phi_{2m}} \quad (55)$$

which is clearly always negative. The derivative of $h_m(\gamma)$ over $\gamma_n, \forall n \in [1, N], n \neq m$ is

$$\frac{\partial h_m(\gamma)}{\partial\gamma_n}$$

$$= \frac{-2\operatorname{Re}(\phi_{1m}^H\Sigma_{\mathbf{Y}_1}^{-1}\mathbf{Y}_1\mathbf{Y}_1^H\Sigma_{\mathbf{Y}_1}^{-1}\phi_{1n}\phi_{1n}^H\Sigma_{\mathbf{Y}_1}^{-1}\phi_{1m})}{L\phi_{1m}^H\mathbf{R}_1^{-1}\phi_{1m} + L\phi_{2m}^H\mathbf{R}_2^{-1}\phi_{2m}}$$

$$\times(1 - \gamma_m\phi_{1m}^H\Sigma_{\mathbf{Y}_1}^{-1}\phi_{1m})$$

$$+ \frac{\gamma_m\left\|\mathbf{Y}_1^H\Sigma_{\mathbf{Y}_1}^{-1}\phi_{1m}\right\|_2^2\left\|\phi_{1m}^H\Sigma_{\mathbf{Y}_1}^{-1}\phi_{1n}\right\|_2^2}{L\phi_{1m}^H\mathbf{R}_1^{-1}\phi_{1m} + L\phi_{2m}^H\mathbf{R}_2^{-1}\phi_{2m}}$$

$$+ \frac{-2\operatorname{Re}(\phi_{2m}^H\Sigma_{\mathbf{Y}_2}^{-1}\mathbf{Y}_2\mathbf{Y}_2^H\Sigma_{\mathbf{Y}_2}^{-1}\phi_{2n}\phi_{2n}^H\Sigma_{\mathbf{Y}_2}^{-1}\phi_{2m})}{L\phi_{1m}^H\mathbf{R}_1^{-1}\phi_{1m} + L\phi_{2m}^H\mathbf{R}_2^{-1}\phi_{2m}}$$

$$\times(1 - \gamma_m\phi_{2m}^H\Sigma_{\mathbf{Y}_2}^{-1}\phi_{2m})$$

$$+ \frac{\gamma_m\left\|\mathbf{Y}_2^H\Sigma_{\mathbf{Y}_2}^{-1}\phi_{2m}\right\|_2^2\left\|\phi_{2m}^H\Sigma_{\mathbf{Y}_2}^{-1}\phi_{2n}\right\|_2^2}{L\phi_{1m}^H\mathbf{R}_1^{-1}\phi_{1m} + L\phi_{2m}^H\mathbf{R}_2^{-1}\phi_{2m}} \quad (56)$$

Denote a set $\mathbb{M}$ that contains the indexes that correspond to the target directions in the dictionary and the optimal point as γ^*. Then one can easily get:

$$h(\gamma_m^*) = \begin{cases} 1, & \text{if } m \notin \mathbb{M} \\ 1 - \gamma_m^*\frac{(\phi_{1m}^H\mathbf{R}_1^{-1}\phi_{1m})^2 + (\phi_{2m}^H\mathbf{R}_2^{-1}\phi_{2m})^2}{\phi_{1m}^H\mathbf{R}_1^{-1}\phi_{1m} + \phi_{2m}^H\mathbf{R}_2^{-1}\phi_{2m}}, & \text{otherwise} \end{cases} \quad (57)$$

If $m \notin \mathbb{M}$, one can obtain the following result from (55) and (56):

$$\left.\frac{\partial h_m(\gamma)}{\partial\gamma_m}\right|_{\gamma=\gamma^*} \leq 0, \forall m \in [1, N] \quad (58)$$

where $(\cdot)|_{\gamma=\gamma^*}$ represents the value at $\gamma = \gamma^*$. Since the derivative of h_m is also continuous, it can be seen that

$$\exists \delta_1 > 0, s.t. h_m(\gamma) \leq 1, \forall \gamma \in [\gamma^*, \gamma^* + \delta_1] \quad (59)$$

If $m \in \mathbb{M}$, $h_m(\gamma^*) < 1$. Thus it can be obtained that

$$\exists \delta_2, s.t. h_m(\gamma) \leq 1, \forall |\gamma - \gamma^*| \leq \delta_2 \quad (60)$$

Combining (59) and (60), we can get that

$$\forall m \in [1, N], \exists \delta > 0,$$
$$s.t. 0 \leq h_m(\gamma) \leq 1, \forall \gamma \in \mathbb{K} = \{\gamma | \delta \geq \gamma_m - \gamma_m^* \geq 0\} \quad (61)$$

Therefore, if the initial point of the iteration belongs to the set $\mathbb{K}$, one can obtain from (61) that

$$0 \leq \gamma_m^{j+1} - \gamma_m^* < \gamma_m^j - \gamma_m^*, \forall m \in [1, N], j \geq 0 \quad (62)$$

which is a direct result from the Lagrange Mean Value Theorem and $h_m \geq 0$. Therefore, we can see that provided the initial point is already close to the optima, the sequence γ would always converge to the optimal point. ■

APPENDIX C
PROOF OF LEMMA 1

Proof: The derivative of $g(\gamma_m)$ over γ_m is

$$\frac{\partial g(\gamma_m)}{\partial\gamma_m} = \phi_{im}^H\Sigma_{\mathbf{Y}_i}^{-1}\phi_{im}(1 - \gamma_m\phi_{im}^H\Sigma_{\mathbf{Y}_i}^{-1}\phi_{im}) \quad (63)$$

Since $\Sigma_{\mathbf{Y}_i}^{-1}$ is always positive semi-definite, $\phi_{im}^H\Sigma_{\mathbf{Y}_i}^{-1}\phi_{im} > 0$. From (63), we can see that

$$\begin{cases} \frac{\partial g}{\partial\gamma_m} > 0, & \text{if} \gamma_m\phi_{im}^H\Sigma_{\mathbf{Y}_i}^{-1}\phi_{im} < 1 \\ \frac{\partial g}{\partial\gamma_m} = 0, & \text{if} \gamma_m\phi_{im}^H\Sigma_{\mathbf{Y}_i}^{-1}\phi_{im} = 1 \\ \frac{\partial g}{\partial\gamma_m} < 0, & \text{if} \gamma_m\phi_{im}^H\Sigma_{\mathbf{Y}_i}^{-1}\phi_{im} > 1 \end{cases} \quad (64)$$

Let us first consider the case that $max(\gamma_m)$ exists on the domain $\mathbb{R}^+$ and the it is achieved at γ_m' that satisfies $g(\gamma_m') > 1$. Since the inversion of a positive semi-definite matrix is continuous about its elements, the function $g(\gamma_m)$

is also a continuous function. According to the property of continuous function, for an arbitrary $\epsilon > 0$, there exists a δ such that whenever $|\gamma_m - \gamma'_m| < \delta$, $|g(\gamma_m) - g(\gamma'_m)| < \epsilon$. Let $\epsilon < |g(\gamma'_m) - 1|$, then on the interval $[\gamma'_m - \delta, \ \gamma'_m)$, we have $g(\gamma_m) > 1$ and $\frac{\partial g}{\partial \gamma_m} < 0$. Because of the continuity, we have

$$\lim_{\gamma_m \to (\gamma'_m)^-} g(\gamma_m) = g(\gamma'_m) \tag{65}$$

According to the assumption, it can be obtained that

$$\exists \overline{\gamma}_m \in [\gamma'_m - \delta, \ \gamma'_m), \ s.t. \lim_{\gamma_m \to (\gamma'_m)^-} g(\gamma_m) > g(\overline{\gamma}_m) \tag{66}$$

Then, in a small $\delta'-$ neighborhood of γ'_m, we have $g(\gamma_m) > g(\overline{\gamma}_m)$ which clearly contradicts the conclusion that on the interval $[\gamma'_m - \delta, \ \gamma'_m)$, the function $g(\gamma_m)$ is monotonically decreasing.

Consider the case that $max(\gamma_m)$ does not exist on the domain $\mathbb{R}^+$. If $\sup(g(\gamma_m)) > 1$, there exists a point γ'_m such that $g(\gamma'_m) > 1$. Then from the above analysis, there exists an interval $[\gamma'_m - \delta, \ \gamma'_m)$ such that every point on the interval satisfies $g(\gamma_m) > g(\gamma'_m)$. Continuing this derivation, we could obtain that

$$\lim_{\gamma_m \to (0)^+} g(\gamma_m) > 0 \tag{67}$$

which contradicts the continuity at $\gamma_m = 0$.

Therefore, it could be obtained that $\sup(g(\gamma_m)) \leq 1$. ∎

REFERENCES

[1] K. Zarifi and A. B. Gershman, "Generalized correlation decomposition-based blind channel estimation in DS-CDMA systems with unknown wide-sense stationary noise," *IEEE Trans. Signal Process.*, vol. 56, no. 11, pp. 5605–5617, Nov. 2008.

[2] C. Qian, L. Huang, N. D. Sidiropoulos, and H. C. So, "Enhanced PUMA for direction-of-arrival estimation and its performance analysis," *IEEE Trans. Signal Process.*, vol. 64, no. 16, pp. 4127–4137, Aug. 2016.

[3] M. M. Nikolic, A. Nehorai, and A. R. Djordjevic, "Estimation of direction of arrival using multipath on array platforms," *IEEE Trans. Antennas Propag.*, vol. 60, no. 7, pp. 3444–3454, Jul. 2012.

[4] U. Nickel, "Overview of generalized monopulse estimation," *IEEE Aerosp. Electron. Syst. Mag.*, vol. 21, no. 6, pp. 27–56, Jun. 2006.

[5] F. G. Yan, M. Jin, S. Liu, and X. L. Qiao, "Real-valued MUSIC for efficient direction estimation with arbitrary array geometries," *IEEE Trans. Signal Process.*, vol. 62, no. 6, pp. 1548–1560, Mar. 2014.

[6] X. Zhang, Y. Huang, C. Chen, J. Li, and D. Xu, "Reduced-complexity capon for direction of arrival estimation in a monostatic multiple-input multiple-output radar," *IET Radar, Sonar, Navigat.*, vol. 6, no. 8, pp. 796–801, Oct. 2012.

[7] C. Qian, L. Huang, and H. C. So, "Improved unitary root-MUSIC for DOA estimation based on pseudo-noise resampling," *IEEE Signal Process. Lett.*, vol. 21, no. 2, pp. 140–144, Feb. 2014.

[8] W. Suleiman, M. Pesavento, and A. M. Zoubir, "Performance analysis of the decentralized eigendecomposition and ESPRIT algorithm," *IEEE Trans. Signal Process.*, vol. 64, no. 9, pp. 2375–2386, May 2016.

[9] H. Krim and M. Viberg, "Two decades of array signal processing research: The parametric approach," *IEEE Signal Process. Mag.*, vol. 13, no. 4, pp. 67–94, Jul. 1996.

[10] J.-W. Jhang and Y.-H. Huang, "A high-SNR projection-based atom selection OMP processor for compressive sensing," *IEEE Trans. Very Large Scale Integr. (VLSI) Syst.*, vol. 24, no. 12, pp. 3477–3488, Dec. 2016.

[11] B. D. Jeffs, "Sparse inverse solution methods for signal and image processing applications," in *Proc. IEEE Int. Conf. Acoust., Speech Signal Process.*, vol. 3, May 1998, pp. 1885–1888.

[12] I. F. Gorodnitsky and B. D. Rao, "Sparse signal reconstruction from limited data using FOCUSS: A re-weighted minimum norm algorithm," *IEEE Trans. Signal Process.*, vol. 45, no. 3, pp. 600–616, Mar. 1997.

[13] B. D. Rao and K. Kreutz-Delgado, "An affine scaling methodology for best basis selection," *IEEE Trans. Signal Process.*, vol. 47, no. 1, pp. 187–200, Jan. 1999.

[14] D. P. Wipf and B. D. Rao, "An empirical Bayesian strategy for solving the simultaneous sparse approximation problem," *IEEE Trans. Signal Process.*, vol. 55, no. 7, pp. 3704–3716, Jul. 2007.

[15] D. Malioutov, M. Çetin, and A. S. Willsky, "A sparse signal reconstruction perspective for source localization with sensor arrays," *IEEE Trans. Signal Process.*, vol. 53, no. 8, pp. 3010–3022, Aug. 2005.

[16] P. Gerstoft, A. Xenaki, and C. F. Mecklenbrauker, "Multiple and single snapshot compressive beamforming," *J. Acoust. Soc. Amer.*, vol. 138, no. 4, pp. 2003–2014, Oct. 2015.

[17] S. F. Cotter, B. D. Rao, K. Engan, and K. Kreutz-Delgado, "Sparse solutions to linear inverse problems with multiple measurement vectors," *IEEE Trans. Signal Process.*, vol. 53, no. 7, pp. 2477–2488, Jul. 2005.

[18] T. Hastie, R. Tibshirani, and J. Friedman, *The Elements of Statistical Learning*, New York, NY, USA: Springer, 2001.

[19] J. Chen and X. Huo, "Sparse representations for multiple measurement vectors (MMV) in an overcomplete dictionary," in *Proc. IEEE Int. Conf. Acoust., Speech, Signal Process. (ICASSP)*, vol. 4. Mar. 2005, pp. 257–260.

[20] J. A. Tropp, "Algorithms for simultaneous sparse approximation. Part II: Convex relaxation," *Signal Process.*, vol. 86, no. 3, pp. 589–602, Mar. 2006.

[21] D. P. Wipf and B. D. Rao, "Latent variable Bayesian models for promoting sparsity," *IEEE Trans. Inf. Theory*, vol. 57, no. 9, pp. 6236–6255, Sep. 2011.

[22] L. Wang, L. Zhao, G. Bi, C. Wan, L. Zhang, and H. Zhang, "Novel wideband DOA estimation based on sparse Bayesian learning with Dirichlet process priors," *IEEE Trans. Signal Process.*, vol. 64, no. 2, pp. 275–289, Jan. 2016.

[23] J. Dai, X. Bao, W. Xu, and C. Chang, "Root sparse Bayesian learning for off-grid DOA estimation," *IEEE Signal Process. Lett.*, vol. 24, no. 1, pp. 46–50, Jan. 2017.

[24] N. Hu, B. Sun, Y. Zhang, J. Dai, J. Wang, and C. Chang, "Underdetermined DOA estimation method for wideband signals using joint nonnegative sparse Bayesian learning," *IEEE Signal Process. Lett.*, vol. 24, no. 5, pp. 535–539, May 2017.

[25] J. Dai and H. C. So, "Sparse Bayesian learning approach for outlier-resistant direction-of-arrival estimation," *IEEE Trans. Signal Process.*, vol. 66, no. 3, pp. 744–756, Feb. 2018.

[26] L. Zheng and X. Wang, "Super-resolution delay-Doppler estimation for OFDM passive radar," *IEEE Trans. Signal Process.*, vol. 65, no. 9, pp. 2197–2210, May 2017.

[27] P. Lombardo and F. Colone, "Advanced processing methods for passive bistatic radar systems," in *Principles of Modern Radar: Advanced Techniques*, W. L. Melvin and J. A. Scheer, Eds. Rijeka, Croatia: SciTech Publishing, 2012.

[28] A. Farina and H. Kuschel, "Guest editorial special issue on passive radar (Part I)," *IEEE Aerosp. Electron. Syst. Mag.*, vol. 27, no. 10, p. 5, Oct. 2012.

[29] C. Kreucher, "Exploiting narrowband bistatic radar measurements for dismount detection and tracking [measurements corner]," *IEEE Antennas Propag. Mag.*, vol. 53, no. 1, pp. 98–105, Feb. 2011.

[30] E. Hanusa, D. Krout, and M. R. Gupta, "Estimation of position from multistatic Doppler measurements," in *Proc. 13th Int. Conf. Inf. Fusion*, Jul. 2010, pp. 1–7.

[31] Q. Wu, Y. D. Zhang, M. G. Amin, and B. Himed, "Space-Time adaptive processing and motion parameter estimation in multistatic passive radar using sparse Bayesian learning," *IEEE Trans. Geosci. Remote Sens.*, vol. 54, no. 2, pp. 944–957, Feb. 2016.

[32] H. L. van Trees, K. L. Bell, and Y. Wang, "Bayesian cramer-rao bounds for multistatic radar," in *Proc. Int. Waveform Diversity Design Conf.*, Lihue, HI, USA, Jan. 2006, pp. 1–4.

[33] F. Chen, J. Zheng, and J. Dai, "DOD and DOA estimation for bistatic MIMO radars with sparse Bayesian learning," in *Proc. Int. Workshop Antenna Technol. (iWAT)*, Nanjing, China, Mar. 2018, pp. 1–4.

[34] D. Tollefsen, P. Gerstoft, and W. S. Hodgkiss, "Multiple-array passive acoustic source localization in shallow water," *J. Acoust. Soc. America*, vol. 141, no. 3, pp. 1501–1513, Jan. 2017.

[35] J. Chen and X. Huo, "Theoretical results on sparse representations of multiple-measurement vectors," *IEEE Trans. Signal Process.*, vol. 54, no. 12, pp. 4634–4643, Dec. 2006.

[36] F. Colone, P. Falcone, C. Bongioanni, and P. Lombardo, "WiFi-based passive bistatic RADAR: Data processing schemes and experimental results," *IEEE Trans. Aerosp. Electron. Syst.*, vol. 48, no. 2, pp. 1061–1079, Apr. 2012.

[37] K. Chetty, G. E. Smith, and K. Woodbridge, "Through-the-wall sensing of personnel using passive bistatic WiFi radar at standoff distances," *IEEE Trans. Geosci. Remote Sens.*, vol. 50, no. 4, pp. 1218–1226, Apr. 2012.

[38] P. Falcone, F. Colone, and P. Lombardo, "Potentialities and challenges of WiFi-based passive radar," *IEEE Aerosp. Electron. Syst. Mag.*, vol. 27, no. 11, pp. 15–26, Nov. 2012.

[39] P. Falcone, F. Colone, A. Macera, and P. Lombardo, "Two-dimensional location of moving targets within local areas using WiFi-based multistatic passive radar," *IET Radar, Sonar Navigat.*, vol. 8, no. 2, pp. 123–131, Feb. 2014.

[40] C. M. Bishop, *Pattern Recognition and Machine Learning*, New York, NY, USA: Springer, 2006.

[41] X. Zhang, Y. Li, X. Yang, T. Long, and L. Zheng, "Sub-array weighting UN-MUSIC: A unified framework and optimal weighting strategy," *IEEE Signal Process. Lett.*, vol. 21, no. 7, pp. 871–874, Jul. 2014.

[42] M. E. Tipping, "Sparse Bayesian learning and the relevance vector machine," *J. Mach. Learn. Res.*, vol. 1, pp. 211–244, Sep. 2001.

[43] D. J. C. MacKay, "Bayesian interpolation," *Neural Comput.*, vol. 4, no. 3, pp. 415–447, 1992.

[44] P. Stoica and Y. Selen, "Model-order selection: A review of information criterion rules," *IEEE Signal Process. Mag.*, vol. 21, no. 4, pp. 36–47, Jul. 2004.

[45] C. D. Austin, R. L. Moses, J. N. Ash, and E. Ertin, "On the relation between sparse reconstruction and parameter estimation with model order selection," *IEEE J. Sel. Topics Signal Process.*, vol. 4, no. 3, pp. 560–570, Jun. 2010.

[46] Z.-M. Liu, Z.-T. Huang, and Y.-Y. Zhou, "An efficient maximum likelihood method for direction-of-arrival estimation via sparse Bayesian learning," *IEEE Trans. Wireless Commun.*, vol. 11, no. 10, pp. 3607–3617, Oct. 2012.

[47] P. Gerstoft, C. F. Mecklenbrauker, A. Xenaki, and S. Nannuru, "Multi-snapshot sparse Bayesian learning for DOA," *IEEE Signal Process. Lett.*, vol. 23, no. 10, pp. 1469–1473, Oct. 2016.

[48] Z.-M. Liu, "Direction-of-arrival estimation with time-varying arrays via Bayesian multitask learning," *IEEE Trans. Veh. Technol.*, vol. 63, no. 8, pp. 3762–3773, Oct. 2014.

[49] Z. Yang, L. Xie, and C. Zhang, "Off-grid direction of arrival estimation using sparse Bayesian inference," *IEEE Trans. Signal Process.*, vol. 61, no. 1, pp. 38–43, Jan. 2013.

[50] D. H. Brandwood, "A complex gradient operator and its application in adaptive array theory," *IEE Proc. F Commun., Radar Signal Process.*, vol. 130, no. 1, pp. 11–16, Feb. 1983.

XINYU ZHANG received the B.S. and Ph.D. degrees from the Beijing Institute of Technology, in 2011 and 2017, respectively. He visited The Ohio State University, from 2015 to 2017, as a Visiting Scholar. Since 2017, he has been holding a postdoctoral position with the National University of Defense Technology, where he is currently a Lecturer with the College of Electronic Science and Engineering. He is the author of more than 11 papers and holds two patents. His current research interests include array signal processing, auto target detection, and waveform optimization.

KAI HUO was born in Hubei, China, in 1983. He received the B.S. degree in communication engineering and the Ph.D. degree in electronic science and technology from the National University of Defense Technology (NUDT), China, in 2005 and 2011, respectively, where he is currently a Lecturer. His research interests include radar signal processing and feature extraction.

YONGXIANG LIU received the B.S. and Ph.D. degrees from the National University of Defense Technology (NUDT), in 1999 and 2004, respectively. In 2008, he was an Academic Visitor with Imperial College London. Since 2004, he has been with NUDT, where he is currently a Professor with the College of Electrical Science and Engineering, conducting research on radar target recognition, time–frequency analysis and micro-motions, and array signal processing.

XIANG LI received the B.S. degree from Xidian University, Xi'an, in 1989, and the M.S. and Ph.D. degrees from the National University of Defense Technology, in 1995 and 1998, respectively. He is currently a Professor with the National University of Defense Technology and performs research on array signal processing, auto target recognition, signal detection, and non-linear signal processing. He has published more than 200 papers and five monographs and holds 13 patents.

• • •